



Performance of evacuated tube solar collector integrated solar desalination unit – a review

Rajeev Kumar^{a,*}, Desh Bandhu Singh^b, Ashish Dewangan^c, Vivek Kumar Singh^d, Navneet Kumar^c

^aDepartment of Mechanical Engineering, Government Polytechnic, UT Administration of DNH and DD, Daman-396210, India, email: rajeevkumar002@gmail.com

^bDepartment of Mechanical Engineering, Graphic Era Deemed to be University, Clement town, Dehradun Uttarakhand-248002, India, email: deshbandhusingh.me@geu.ac.in

^cGalgotias College of Engineering and Technology Greater Noida-201306, UP, India, emails: ashishdewangan0515@gmail.com (A. Dewangan), navneet_mech48@yahoo.com (N. Kumar)

^dEnergy for Sustainability Initiative, University of Coimbra, Portugal, email: vivekkumarsingh22@gmail.com

Received 6 June 2018; Accepted 27 April 2021

ABSTRACT

Low-cost potable water is a challenge nowadays and research are going on based on the solar thermal technique in order to bring down the cost of yield worldwide. The evacuated tubular collector is generally used to achieve higher collector efficiency. A higher rate of vaporization is achieved by integrating a number of series-connected evacuated tubes with solar still. In this work, the effect of heat transfer rate on the performance of evacuated tubular collector systems and natural evaporation and condensation-based freshwater yield in free and forced modes is reviewed. The performance of the evacuated tube is affected by varying tilt angles and an increase in the intensity of solar radiation. The overall performance of the system depends on the heat transfer rate from the absorber tube to the working fluid. The heat transfer rate can further be improved by adding various sizes of nanoparticles to working fluid and act as a heat-absorbing device during less sunshine or cloudy days. Previous finding such as operating temperature and flow behavior inside evacuated tube collector, daily freshwater yield variation with respect to depth of water inside solar still, system efficiency of the integrated system and variation in energy and exergy efficiency are presented step by step throughout the paper.

Keywords: Active solar still; Evacuated tubular collector; Exergy; Nanofluid

1. Introduction

Solar distillation of saline/brackish water is an attractive alternative to obtain fresh water. Solar flux is transmitted inside the enclosure of the distillation unit and reaches the blackened surface (basin liner) and thermal energy is convected to water mass. The evaporative water gets condensed on the inner surface of the glass cover and gets collected at the lower end of the glass cover. A solar

distillation system is used to get freshwater from vapor by absorbing solar radiation. This vapor gets condensed along with the glass cover and trickles down the channel which in turn gets collected in a jar for use. A collector is a device that converts the radiation (beam/diffuse) from incoming sunlight into useful heat energy; however, this collection/conversion efficiency is less because of entropy gain to the environment. Glass evacuated collector is widely used nowadays for solar thermal utilization. Producing hot water using an evacuated tube collector (ETC) is more popular because of its tubular shape. Hot

* Corresponding author.

water can be utilized for domestic as well as industrial purposes such as textile, leather, paper industries, etc. ETC is used in combination with solar still to improve the yield of freshwater. Still is of two types: passive and active solar still. Active still requires other heat-absorbing collectors as compared to passive solar still which use solar radiation directly to evaporate water. In the indirect type of solar desalination system, the additional solar thermal collector is used to collect the solar energy to improve potable water yield. Figs. 1 and 2 show the schematic diagram of passive and active solar still respectively [1].

Multi-effect distillation, multi-stage flash desalination, thermal vapor compression, mechanical vapor compression and reverse osmosis utilize a conventional source of energy for potable water production whereas solar still uses a non-conventional source of energy [2].

2. Classification

2.1. Solar still

Compound parabolic concentrator concentric tubular solar still was integrated to single slope and pyramid type solar still, the productivity is slightly higher for pyramid solar still as compared to single slope solar still because the

area is more for pyramid still [3]. According to Tiwari [4], solar still is classified as:

- (a) Passive solar still
 - Single slope still
 - Double slope still
 - Symmetrical
 - Non-symmetrical
- (b) Active solar still
 - High-temperature distillation
 - Auxiliary heating distillation
 - Distillation with collector/concentrator
 - Nocturnal distillation

The performance is evaluated for three different modified designs of single slope solar still-simple flat basin with the interior reflecting mirror, Stepwise basin solar still and coupling step-wise basin with a sun tracking system. The later design provides more surface area and maintains maximum temperature for a longer period [5]. The work is reviewed by various researcher related to solar still and showed that its efficiency depends on the following parameters: cover plate temperature, convective heat transfer from side walls and cover plate, coating,

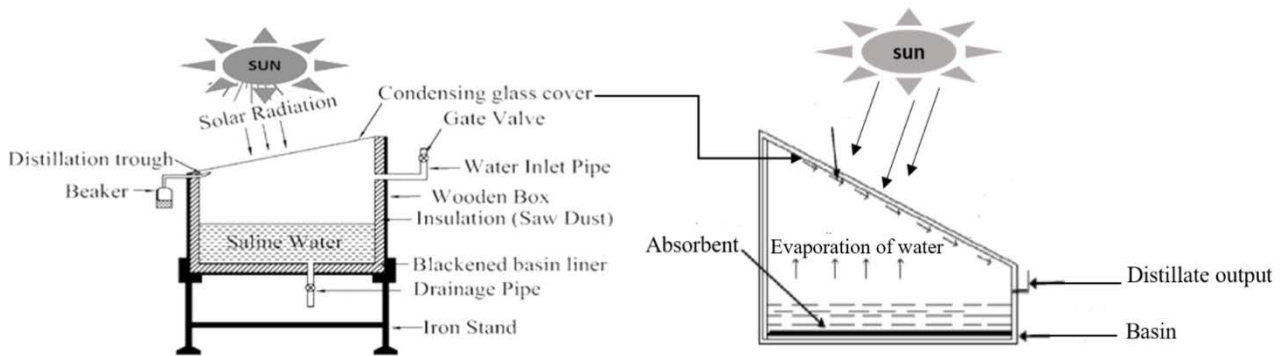


Fig. 1. Schematic of passive solar still adapted from the study of Sampathkumar et al. [1].

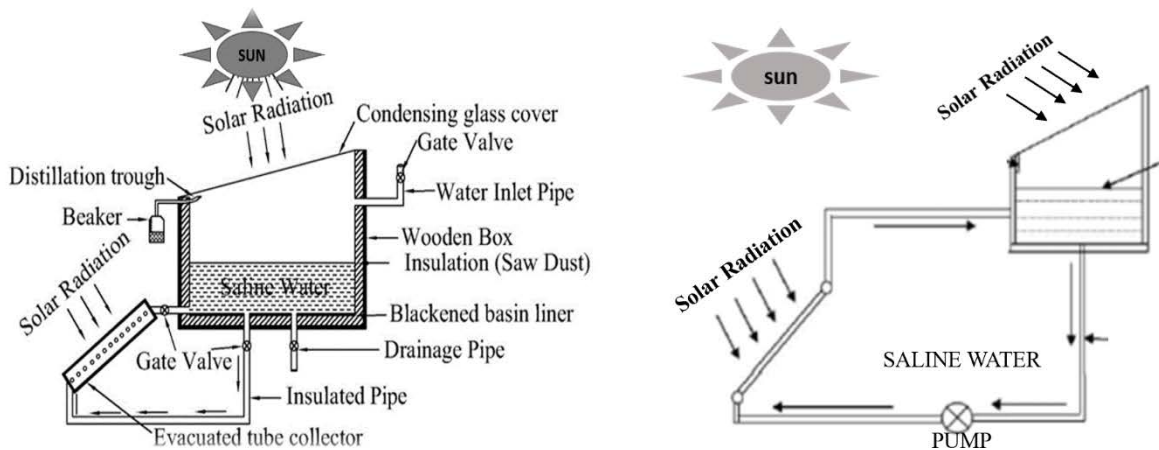


Fig. 2. Schematic of active solar still adapted from the study of Sampathkumar et al. [1].

design of shapes and structure, depth of water, external enhancement, feedwater flow rate, the orientation of solar still, solar tracking and tilt angle of cover plate [6]. Various techniques were incorporated by many researchers to improve the yield and efficiency of solar still included with ETC [7], pulsating heat pipe [8], parabolic trough [9], flat plate collector [10], the thermoelectric effect [11], etc.

Low and medium temperature application such as water heating, desalination, etc is achieved by non-concentrating collectors and high temperature is achieved by concentrating solar collector [12]. The radiation flux increases on the smaller receiver area because of the concave reflecting surface which intercepts beam radiation in the case of concentrating collector [13]. Lists of various special designs of solar stills namely concave wick solar still, spherical solar still, hemispherical solar still, tubular solar still, compound parabolic concentrator-tubular solar still (CPC-TSS), V-type solar still and pyramid shape solar still. It was concluded that the productivity for CPC-TSS was maximum (large condensation surface) and inverted solar still gave double yield as compared to conventional solar still (CSS) because the radiation is concentrated on the inverted absorber plate [14]. The daily yield is 30% higher in winter and 3% higher in summer for a single slope than pyramid still due to radiation loss from the cover surface. Productivity of pyramid still is lower as compared to single and double slope still because orientation has no effect on productivity [15].

The evaporation rate is augmented for single basin solar still by 15.3%, 29.6% and 45.5% by using sponge, wick and fin (at bottom of still) respectively as compared to simple still. In the case of sponge and wick only surface area is increased but in the case of fin surface area as well as the water temperature is increased [16]. The performance of single basin solar still is evaluated with the optimum tilt angle of glass cover of 33.3° for both summer and winter with an efficiency of 30.65% [17]. The increase in evaporative exergy fraction and efficiency is reported for solar still while convective exergy fraction and radiative exergy fraction decrease with an increase in water temperature. The preferable operating condition to operate solar still is above 30°C. Fractional exergy is the upward exergy transfer by evaporation, convection or radiation from the hot water surface to condensing glass cover within the solar still [18].

2.2. Evacuated tube collector

Heat extraction efficiencies are higher for ETC because of vacuum insulation and high selective surface. Heat energy collected by ETC is 189.33 kWh/m² more when energy performance analysis is done for flat plate collector (FPC) and ETC system [19]. Comparison of single-ended water in glass tubes is done with FPC for reasonable tube size of ETC and found ETC as an alternative to flat plate collector [20]. Radiation and convection losses are minimized by using ETC [21]. The classification of evacuated tube collector has been given below was given by Tiwari [4]:

(c) With heat pipe

- Cusp reflector within the tube
- Metal fin within the tube

(d) Without heat pipe

- Without reflector
 - Evacuated tube cover
 - Single straight tube
 - U-shaped tube manifold
 - U-shaped with insulation
- With reflector
 - Within the evacuated tube
 - Behind evacuated tube or cusp reflector

FPC operates between the temperature range of 20°C–80°C whereas the operating temperature range for ETC is in between 50°C–200°C. In FPC due to the absence of sun-tracking and convection heat loss through the glass cover, the FPC collector gives lower efficiency and outlet temperature.

ETC is of two basic type-single walls evacuated glass tube and Dewar tube. The Dewar tube consists of the inner and the outer tube and the space between these concentric tubes is evacuated [22–24]. The performance of an all-glass vacuum tube is evaluated with coaxial fluid and antifreeze solution through a one-dimensional mathematical model [25]. Available types of the evacuated tubular collector which are used widely are fluid-in-glass and fluid-in-metal. The latter design withstands high pressure and temperature [26]. Water-in-glass ETC, U-type ETC and heat pipe are the three broad classifications of ETC. In a water-in-glass evacuated tube solar collector, the inner tube is filled with water and the outside wall of each inner tube is treated with an absorbent selective coating. In heat-pipe evacuated tube solar collector, evacuated pipe partially filled with a working fluid. In a U-type evacuated tube solar collector, U-tube is inserted inside the inner tube [27]. Comparison of thermal performance of U-tube is done with fin in various shapes. They compared the thermal performance of ETC for four different geometry of absorber tube with fin, U-tube with circular fin, U-tube with copper fin and U-tube inside a rectangular duct. U-tube with a circular fin gave the best performance when a single collector tube was used, and only beam radiation was taken into consideration. Cross-section of different geometry is shown in Figs. 3–6 respectively. They also found that the thermal behavior of tubular collectors depends on the shape of the absorber tube, collector tube center distance (shadow effect) and diffuse radiation [28]. The heat pipe is a two-phase heat transfer device that consists of three section evaporator, adiabatic section and condenser [29].

Circular shapes of vacuum tubes give better performance and are suitable for both direct and diffuse radiation. A cross-section of ETC consisting of outer and inner glass with a U-tube is shown in Fig. 7 [30].

There are several systems that can be attached to ETC for improved thermal output: Stirling engine for solar thermal energy generation is integrated with concentrated ETC [31], solar dryer for agriculture and marine products with ETC [32,33]. Solar cooker based on ETC [34], high-temperature steam generation using ETC [35], ETC as a regenerator for solar air conditioning system [36], hot air production using one-ended ETC [7], solar heat pump for domestic heating with ETC [37–39]. Fluid-in-metal and fluid-in-glass are two basic designs of ETC based on heat

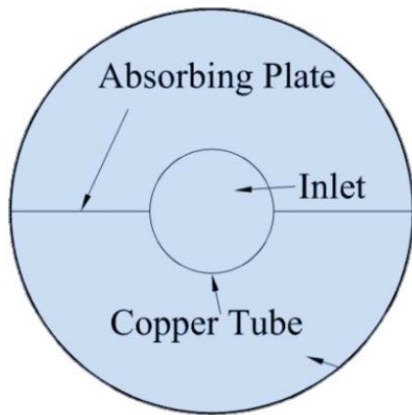


Fig. 3. Cross-sectional of finned tube adapted from the study of Kim and Seo [28].

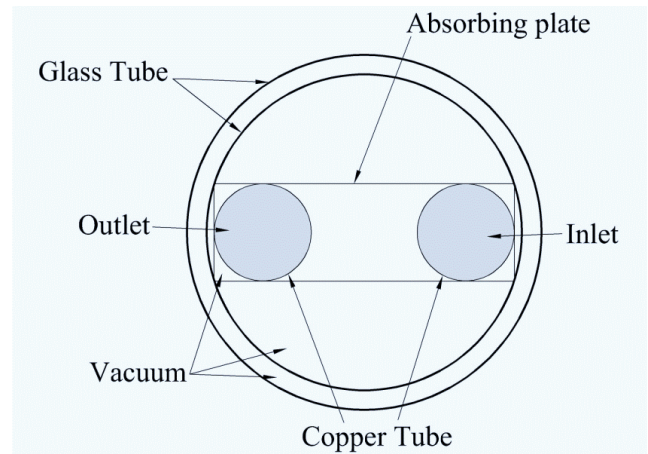


Fig. 6. Cross-section of U-tube inside a rectangular duct adapted from the study of Kim and Seo [28].

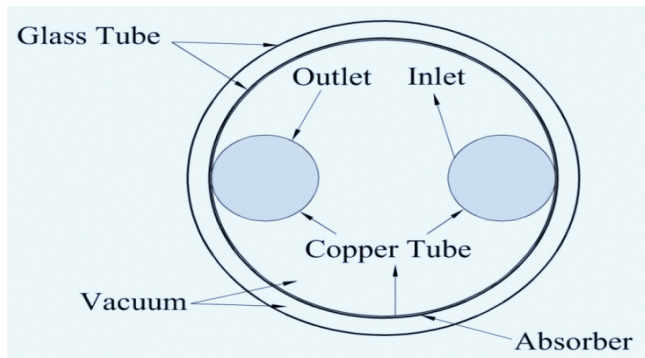


Fig. 4. Cross-section of U-tube inside a circular fin adapted from the study of Kim and Seo [28].

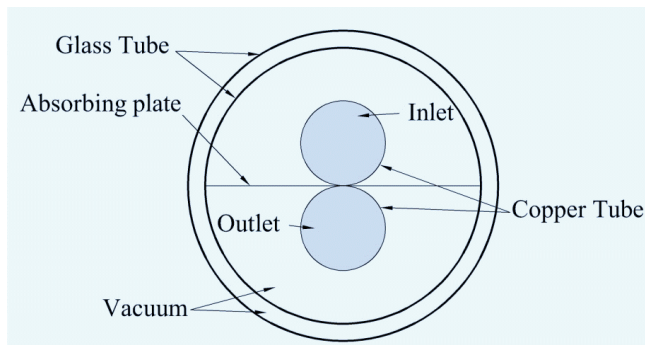


Fig. 5. Cross-section of U-tube on copper plate adapted from the study of Kim and Seo [28].

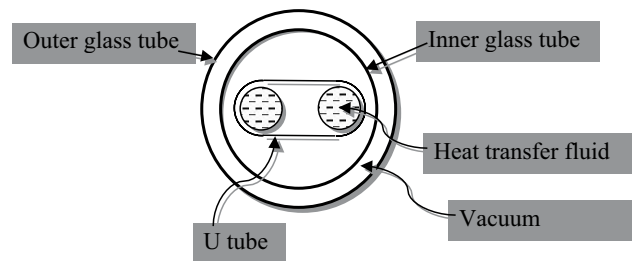


Fig. 7. Cross-sectional of evacuated tubular collector adapted from the study of Singh and Tiwari [87].

extraction, Heat pipe ETC and U-tube glass ETC which is commonly used for domestic water heating are the types of metal-in-glass ETC [40].

Five types of collectors are compared and showed that the instantaneous efficiency of the evacuated solar collector was highest followed by blue coating-selective copper, aluminum, black coating-selective copper and copper solar collector based on absorbed useful heat for a flow rate of 0.033 kg/s [41]. Single envelope vacuum tube with heat pipe is commercialized in Europe and all-glass evacuated

tube with U-tube heat removal is successful in Japan [42]. There are various methods to extract heat from evacuated tubes include heat pipe, flow through the absorber, all-glass tube and storage absorber [43]. The effect of dust deposition on evacuated tube collectors is studied and reported that the potable water yield decreases with a decrease in transmittance of glass tubes [44].

The performance is evaluated for ETC by steady test and quasi-dynamic test methods. For a larger range of operating conditions, higher efficiency was achieved for ETC [45]. The side insulation is used for double basin still and reported that heat loss was less, and the monthly daily average output was increased by 40% as compared to single basin still with sides insulated. He showed that the efficiency of double basin still is higher than single basin still when the tilt angle of the glass cover is taken as 36° and 12° for single basin and double basin solar still respectively [46].

3. Performance parameter

The performance of ETC depends on the absorption of solar radiation, energy transfer from inner glass tube to heat removal fluid and heat lost to the surrounding.

Rayleigh number is the deciding criterion for convection between the inner glass tube and heat transfer fluid:

$$Ra = \frac{g\beta\Delta Tl^3}{\nu\alpha_1} \quad (1)$$

The net heat transfer from the inner glass tube to heat transfer fluid is mainly by radiation and convection. The rate of heat transfer per tube in the radial direction is given by:

$$Q_{\text{cond}} = \frac{2\pi k l_1 (T_s - T_r)}{\ln \frac{d_1}{d_2}} \quad (2)$$

$$Q_{\text{rad}} = \frac{\sigma \pi d_1 l_1 (T_s^4 - T_r^4)}{\frac{1}{\epsilon_r} + \frac{d_1}{d_2} \left(\frac{1}{\epsilon_g} - 1 \right)} \quad (3)$$

Performance reduction occurs if the absorber tube is not in direct contact with heat transfer fluid, hence, the overall efficiency of the combined system depends on the effectiveness of heat transfer [47].

One dimensional analytical investigation is performed for evacuated tube collector with U-tube welded inside a circular fin and studied the effect of air layer and solar intensity on the thermal performance of collector. The effect of thermal resistance of the air layer is considerable on the surface temperature of coating and heat efficiency [48]. The overall heat loss coefficient is calculated for the vacuum collector tube experimentally and a theoretical model is also developed to estimate gas pressure and overall heat loss coefficient [49].

The heat transfer model for all-glass vacuum tube is established in which heat balance equation for the collector is developed by analyzing total solar radiation and internal energy of inlet fluid is taken as input, heat loss and internal energy of outlet fluid is taken as output with assumption. Natural circulation, friction and buoyancy are taken into account for tube and forced circulation in the manifold header. Three experiments were conducted to validate the model, the deviation between predicted and measured result for collector outlet temperature is below 5%. ETCs are employed to enhance heat transfer rate and minimize entropy gain [50].

3.1. Effect of depth of water in still

The effect of water depth is analyzed in active and passive still on internal convective and evaporative heat transfer coefficient [51].

The convective and evaporative heat transfer coefficient is calculated by the expression [52].

$$h_{\text{cw}} = 0.884 \left[(T_w - T_{\text{ci}}) + \frac{(P_w - P_{\text{ci}})(T_w + 273)}{268.9 \times 10^3 - P_w} \right]^{1/3} \quad (4)$$

$$h_{\text{ew}} = \frac{0.01623 k_v}{L_v} C (\text{GrPr})^n \left(\frac{P_w - P_{\text{ci}}}{(T_w - T_{\text{ci}})} \right) \quad (5)$$

where C is the unknown constant in the Nusselt number expression and distillate output is calculated by the expression.

$$\dot{m}_{\text{ew}} = \frac{q_{\text{ew}} A_w t}{L} \quad (6)$$

The convective heat transfer coefficient increases with an increase in depth of water and in active mode evaporative heat transfer coefficient is higher [52]. The depth of water in the distillation unit is analyzed and concluded that the difference between water temperature and inner glass temperature becomes positive for lower depth of water early as compared to the higher depth of water and the water temperature decreases with an increase in water depth and energy is stored in the form of sensible heat. Nocturnal distillation takes place for higher depth. The lower depth of water gives a higher yield during sunshine because of the higher temperature of the evaporative surface and lower temperature of condensing surface [53].

3.2. Efficiency

The thermal efficiency of ETC can be calculated in two ways: Eq. (7) can be used when mass flow rate, inlet and outlet fluid temperature is known and Eq. (8) can be used by considering heat loss while calculating net power output [22].

$$\eta = \frac{\dot{m}_f C_p (T_{\text{out}} - T_{\text{in}})}{A_c G} \quad (7)$$

$$\eta = F_R (\tau \alpha) - \frac{F_R U_L (T_m - T_a)}{G} \quad (8)$$

The overall thermal efficiency of passive and active solar stills was evaluated and can be expressed as [1]:

$$\eta_{\text{passive}} = \frac{m_{\text{ew}} L}{I_s(t) A_s 3,600} \quad (9)$$

$$\eta_{\text{active}} = \frac{m_{\text{ew}} L}{\left((I_c(t) A_c 3,600) + (I_s(t) A_s 3,600) \right)} \quad (10)$$

3.3. Exergy

The available part of certain heat input is exergy and is defined as exergy output to exergy input for still. Exergy output can be increased by decreasing various losses from the still and exergy input is the heat input transferred from the collector after various losses to still, exergy efficiency of evacuated tube integrated still is higher and the hourly thermal exergy output for single slope active solar desalination system can be written as [54].

$$\text{Ex} = A_b h_{\text{ew}} \left[(T_w - T_{\text{gi}}) - (T_a + 273) \times \ln \left\{ \frac{T_w + 273}{T_{\text{gi}} + 273} \right\} \right] \quad (11)$$

The performance of ETC depends on solar flux intensity, incidence angle, slope and orientation of collector, flow rate and thermal properties, fluid inlet temperature and ambient temperature [55].

3.4. Energy payback time

The total energy utilized for the fabrication of an active solar desalination system is known as embodied energy, the time period required to recover this embodied energy is defined as energy payback time (EPBT). Based on energy and exergy the expression can be written as:

$$EPBT(\text{energy}) = \frac{\text{Embodied energy}}{\text{Annual energy output}} = \frac{E_{in}}{E_{out}} \quad (12)$$

$$EPBT(\text{exergy}) = \frac{\text{Embodied energy}}{\text{Annual exergy output}} = \frac{E_{in}}{G_{ex,A}} \quad (13)$$

where E_{in} is embodied energy, $G_{ex,A}$ is overall annual exergy gain and E_{out} is the overall annual energy output [56].

3.5. Energy production factor

The overall performance of active solar desalination system is defined by energy production factor (EPF) and following Tiwari and Mishra it can be expressed as [56]:

$$EPF(\text{energy}) = \frac{E_{out}}{E_{in}} \quad (14)$$

$$EPF(\text{exergy}) = \frac{G_{ex,A}}{E_{in}} \quad (15)$$

3.6. Life cycle conversion efficiencies

The net output of active solar desalination system for its entire lifetime is defined as life cycle conversion efficiency (LCCE) based on energy and exergy and the equation for evaluating this efficiency can be expressed as:

$$LCCE(\text{energy}) = \frac{(E_{out}n - E_{in})}{(E_s n)} \quad (16)$$

$$LCCE(\text{exergy}) = \frac{G_{ex,A}n - E_{in}}{(E_s n)} \quad (17)$$

where n is the life of the system and E_s is the annual solar energy [56].

3.7. Yield

Still performance is measured by the amount of yield and it depends on tilt angle, depth of water, cover plate temperature, etc. Various geometrical variations have been done to improve yield and the amount of yield can be increased by increasing evaporation rate and it depends on the availability of radiation and basin water temperature, the yield quantity is affected by the difference in temperature between basin water and cover temperature [4]. In this paper different type of system is compared for hourly, daily and annual yield.

3.8. Exergoeconomic parameter

It is the method of economic analysis based on exergy, it is the exergy loss per unit cost. Based on energy output, it is expressed as:

$$R_{g,en} = \frac{E_{out}}{UAC} \quad (18)$$

And based on exergy gain:

$$R_{g,ex} = \frac{G_{ex,annual}}{UAC} \quad (19)$$

where $G_{ex,annual}$ is overall yearly exergy gain, E_{out} is overall yearly energy output and UAC is the uniform end of year annual cost of N-PVT-CPC-SS/DS (PVT – Photovoltaic thermal; DS – Double slope) [57].

3.9. Enviroeconomic parameter

The environmental pollution can be reduced and for this economic incentive is provided for using renewable energy technologies and is based on the quantity of emitted carbon and cost of CO₂ emission, based on energy the reduction in CO₂ emission for the whole life of N-PVT-CPC-SS/DS is given by the expression:

$$X_{CO_2,E} = (E_{out} \times n - E_{in}) \times 2 \times 10^{-3} \quad (20)$$

where E_{out} is the annual energy that is available from N-PVT-CPC-SS/DS, E_{in} is embodied energy for N-PVT-CPC-SS/DS and n is the proposed life of the system. Based on exergy the reduction in CO₂ emission for the whole life of N-PVT-CPC-SS/DS is given by the expression:

$$X_{CO_2,Gx} = (G_{ex,annual} \times n - E_{in}) \times 2 \times 10^{-3} \quad (21)$$

where $G_{ex,annual}$ the annual exergy gain and n is the life of N-PVT-CPC-SS/DS [58].

4. Solar desalination unit in combination with evacuated tube collector

The yield from solar still can be increased by integrating it with an evacuated tubular solar collector either in natural mode or forced mode as compared to another collector. Figs. 8 and 9 show the schematic diagrams of single slope solar still integrated evacuated tube collector in natural and forced mode. The fluid flowing through the collector is usually a mixture of water and glycol and the evaporation rate is improved by integrating ETC, FPC, heat pipe and parabolic concentrator with solar still in case of active solar still as compared to low productivity of passive solar still [59].

The experiment is done for the simple solar still (case I) and by coupling an ETC solar water heater with simple solar still (case II) and found that yield from coupled mode is increased by 77% as compared to simple solar still mode for the same still area. The coupled system (case II) is operated for different time period [for 24 h (case A), morning 8–12 h

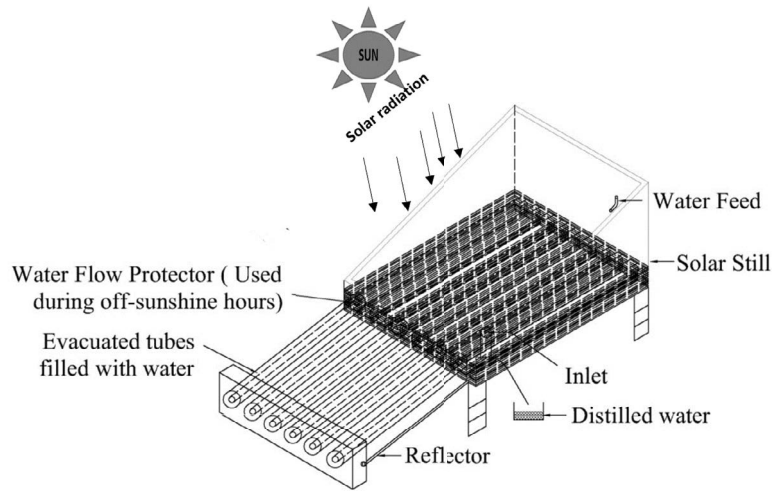


Fig. 8. Schematic diagram of ETC integrated with single slope solar still in a natural mode adapted from the study of Singh et al. [58].

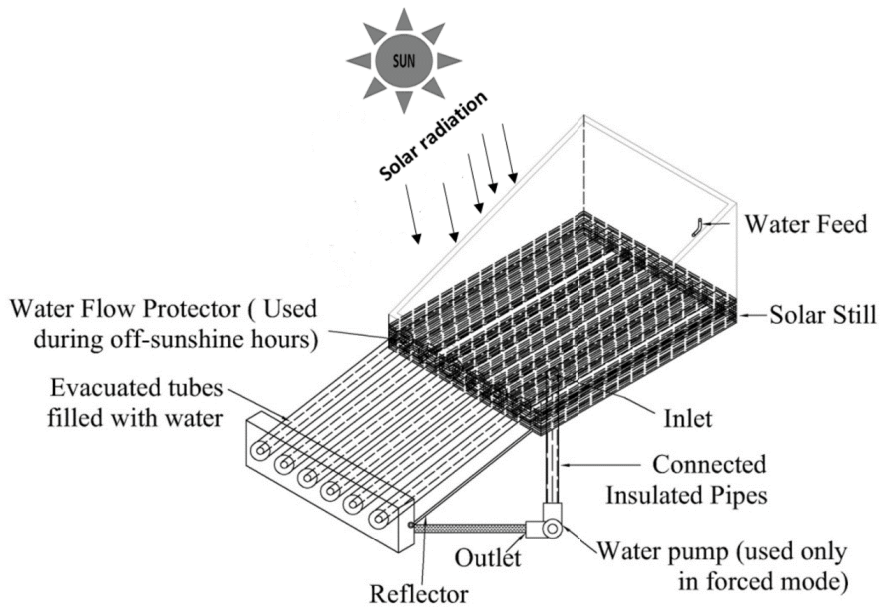


Fig. 9. Schematic diagram of ETC integrated with single slope solar still in forced mode from the study of Zhiqiang et al. [59].

(case B), afternoon hours 12–17 h (case C), during day 8–17 h (case D), still is connected when the water temperature in ETC solar water heater reached 60°C (case E), summer day with rain 8–17 h (case F)], the maximum yield is obtained when still is connected to ETC for 24 h period out of six cases A to F and the calculation of thermal efficiency and solar still yield is done for different cases, the hybrid nature of the system produces hot water and freshwater when ETC solar water heater is coupled with solar still [60]. Table 1 shows some of the recent research findings on solar desalination units in combination with evacuated tube collectors.

A shear layer exists between hot and cold streams in a water-in-glass tube and the boundary layer is the main driving force for fluid movement, cold fluid penetrates down through the core of the tube and drawn toward the boundary layers formed by a heated wall, it swirls near the

bottom sidewalls and forms an outgoing flow, the performance of the tube is affected by stagnation region in the bottom of the long tube [43].

A simplified expression for instantaneous exergy efficiency in terms of energy efficiency is developed for still. When the system is at temperature T , the exergy associated is given as:

$$\dot{E}x = q_u \left(1 - \frac{T_a}{T} \right) \tag{22}$$

The exergy efficiency of passive solar still is given as:

$$\varepsilon = \frac{\text{Exergy output from still}}{\text{Exergy input to still}} = \frac{\dot{E}x_{out}}{\dot{E}x_{in}} = \frac{\dot{E}x_{evaporation}}{\dot{E}x_{sun}} \tag{23}$$

Table 1
Summary of recent previous researches on evacuated tubular solar collector integrated solar desalination unit

Author(s)	Year/Investigation	Type of ETC/ number	Depth (m)	Research findings
Zhiqiang et al. [59]	2012/Experimental (active)	ETSC-SS (forced)	0.05	Maximum water temperature 90.8°C; maximum yield per day 3.328 kg/m ² ; overall thermal efficiency of EISS is 29.9%; annual yield for EISS is more than single slope solar still; cost per kg of still Rs. 6.15
Kumar et al. [60]	2013/Theoretical	ETSC (natural mode)/10	0.03	Basin water temperature 80°C; maximum daily yield of 3.8 kg/m ² ; maximum daily energy and exergy efficiency is 33% and 2.5%
Sampathkumar and Senthilkumar [61]	2013/Experimental	ETC/20 (wick)	0.01, 30°	Distillate output is higher for single layer lined wick (SLLW); daily average still efficiency for single layer plane wick, SLLW and CSS are 66%, 68% and 37.5%, respectively; wick still have higher efficiency than basin still
Omara et al. [62]	2014/Experimental (active)	ETC/5	0.02	Maximum basin water temperature is 83.93°C; maximum production per hour 1.02 kg/m ² ; effect of depth of water in basin is studied; for a unit area of still cost of distillate is 0.0092 \$/L
Jahangiri Mamouri et al. [63]	2016/Theoretical (natural mode)	ETC/10/30	0.07	Maximum yield 2.3 kg/m ² with 10 tubes; variation in temperature for various depth in basin is studied; maximum exergy efficiency 6.86%; maximum daily production is 4.77 kg/m ² with 30 tubes
Yari et al. [64]	2016/Experimental (active)	ETC/2	Half and full ETC	Maximum water temperature 97°C; highest production for full evacuated tube in forced convection is 1.11 kg/m ² h; water basin is not used in this study; hourly efficiency 68% (hourly)
Shafii et al. [65]	2016/Theoretical	ETC	0.01	Water temperature in collector is 87°C; yield is 1.18 kg/h from single solar still and 4.7 kg/h from four solar still (area 4 m ²); daily yield from CSS, single solar still, four solar still, humidification-dehumidification and hybrid solar desalination system is 3.2, 10.5, 42, 24.3 and 66.3 kg, respectively
Sharshir et al. [66]	2017/Theoretical	N-ETC	0.14	Compared daily yield; energy output and exergy efficiency of N-ETC-SS with N-PVT-CPC-SS and CSS

$$\dot{E}x_{\text{evaporation}} = q_{\text{ew}} \left(1 - \frac{T_a}{T_w} \right) \tag{24}$$

The evaporative heat flux is expressed as:

$$q_{\text{ew}} = h_{\text{ew}} A_b (T_w - T_g) \tag{25}$$

And for evaluating exergy of solar radiation the maximum efficiency ratio (exergy to energy ratio) is expressed as:

$$\frac{\dot{E}x_{\text{sun}}}{I_s(t)} = \left[1 - \frac{4}{3} \left(\frac{T_a}{T_s} \right) + \frac{1}{3} \left(\frac{T_a}{T_s} \right)^4 \right] \tag{26}$$

T_s is solar radiation temperature, that is, sun temperature at 6,000 K.

Using Eqs. (22)–(25) the instantaneous exergy efficiency of the passive solar still is expressed as Kumar and Tiwari [18].

$$\varepsilon_i = \eta_i \frac{\left(1 - \frac{T_a}{T_w} \right)}{\left[1 - \frac{4}{3} \left(\frac{T_a}{T_s} \right) + \frac{1}{3} \left(\frac{T_a}{T_s} \right)^4 \right]} \tag{27}$$

where η_i is the instantaneous energy efficiency of passive solar still and it is expressed as:

$$\eta_i = \frac{h_{\text{ew}} (T_w - T_{\text{gi}}) A_b}{I_s(t) A_g} \tag{28}$$

The instantaneous energy of an integrated system can be expressed as Kumar et al. [60].

$$\eta_{\text{ei}} = \frac{h_{\text{ew}} (T_w - T_{\text{gi}}) A_b}{I_s(t) A_b + I_c(t) A_a} \tag{29}$$

The heat extraction efficiency of ETC is evaluated by calculating thermal loss under particular solar flux, mean fluid temperature, ambient temperature and the value of optical efficiency [67]. The highest thermal performance of ETC is achieved by maintaining the tube distance of about 0.2 m and the azimuthal angle of the collector should be about 45°–60° towards the west for vertically placed tubes [68].

A novel distillation system is introduced in which the hourly yield of the active system increases compared to the passive system due to the use of pulsating heat pipe [69]. A computational method is used to study temperature, velocity profile and buoyancy effect inside water-in-glass evacuated tube using Boussinesq approximation and variation of the properties with temperature (VPT) model [8].

4.1. Natural mode

A theoretical model is used for a new passive desalination system in which the production rate increases from 0.83 to 1.01 kg/m² h when the ETC is filled with stainless steel wool to absorb more heat with an inclination angle of 35° when the basin is filled with 80% of water [27]. There is a decrease in hourly yield from 0.564 to 0.424 kg/m² h and daily yield from 3.8 to 3.4 kg/m² with an increase in depth from 0.03 to 0.05 m and he also showed a time difference between maximum radiation and maximum yield due to time lag between evaporation, condensation and storage effect with ten evacuated tubes integrated with single slope still [58]. The thermal model is studied for natural mode still and the result showed the maximum daily yield is 2.3 kg/m² with ten tubes and 4.77 kg/m² with thirty tubes for a depth of 0.07 m, he showed that energy and exergy efficiencies decrease with an increase in a number of tubes which increases heat loss with increase in the surface area [63]. A hybrid solar desalination system is used which consist of wick layers (single and double), wick type (plane wick, lined and square thick linen woven fabric wick), the inclination of wick solar still base and by feeding hot water from ETC solar water heater to the wick still during the night to increase the productivity of distilled water yield [61]. A correlation was developed for natural circulation in terms of solar inputs like tank temperature, the inclination of collector and tube aspect ratio through water in a glass tube mounted over a diffuse reflector [70].

Comparison of filled type evacuated tube solar collector with copper fin evacuated tube collectors is done, the efficiency of filled evacuated tube collector is 77% when the conductivity of heat transfer component is hundred and efficiency is 12% higher than copper fin evacuated tube collector, air thermal resistance is neglected for filled type when heat is transferred from absorber tube to working fluid [50]. An experiment is conducted using nanofluid and showed its effect on the energy efficiency of the collector and concluded that higher natural circulation is obtained because of density gradient and decrease in viscosity when the temperature is increased for lower mass flow rate [71]. Two experiments are performed for two different collector tilt angle of 22° and 46°, in his first experiment he focused on system daily thermal conversion efficiency and in his second experiment he studied

water flow characteristic inside solar tubes for these two angles, the temperature difference between inlet and outlet of the tube is stable throughout the day because of flow is laminar and stable for lower angle and for higher tilt angle temperature difference is lower in the afternoon with intense mixing and heat transfer increases [72]. Monthly, daily and hourly yield is more in active solar still because of additional thermal energy supplied from evacuated tube collectors, hot water temperature in active solar still is 26°C more than passive still at a depth of 0.04 m [1]. Water-in-glass manifold is investigated and showed that at lower flow rate and at lower temperature longitudinal heat flow breaks down when the tubes are vertical results in an increase in glass temperature, the buoyancy effect is also negligible when the inclination is close to horizontal [59].

4.2. Forced mode

The thermal model is studied for ETC in forced mode integrated still shows with an increase in mass flow rate from 0.001 to 0.006 kg/s, the daily yield varies from 2.57 to 3.47 kg/s and water temperature varies from 83.0°C to 92.6°C and he also showed with an increase in basin water depth from 0.01 to 0.05 m, daily yield decreases from 2.60 to 1.58 kg/m², higher daily yield is obtained in forced mode with an optimum mass flow rate of 0.06 kg/s than the natural mode for the same size [60]. The optimum number of evacuated tube collector in ETC-SS and ETC-DS is twelve theoretically for an optimum mass flow rate of 0.016 kg/s, beyond this value slope of the curve between outlet water temperature at the end of *N*th water collector and the number of ETC decreases and overlapped if the mass flow rate is increased further at 0.14 m water depth [57].

For the change in declination angle of sun and inclination angle of ETC and single slope solar still, the total radiation observed in January is higher than May and total yield is higher in summer as compared to winter months because of the low difference between ambient and basin water during summer for evacuated tube collector integrated solar still (single slope) (EISS), the maximum and minimum temperature of water 90.8°C and 56.8°C during June and January respectively with a maximum yield of 3.328 kg/m² in May and a minimum yield of 1.114 kg/m² in December with a depth of 0.5 m for Indian climatic condition [73]. Three experiments are performed and the effect of depth of water in an evacuated tube by eliminating the water basin is studied, the yield was higher for a full evacuated tube with propeller fan followed by a full evacuated and half evacuated tube without propeller fan; the electricity for small propeller fan is generated by using thermoelectric module [6]. The efficiency of solar collectors is compared using supercritical CO₂ and water as a working fluid to heat water, the efficiency is higher when supercritical CO₂ is used as a working fluid as it operates at higher pressure and temperature [74].

FPC and ETC are compared on the basis of energy output, the efficiency of the collector, energy delivered to the hot water tank and heat loss under the same operating and weather condition, the maximum efficiency is 71.4% for ETC and it generated 3.5% more energy than FPC annually, the annual average collector efficiency of ETC is 14.6% more than FPC [19].

5. ETC integrated solar distillation unit loaded with nanofluid

A fluid that contains nanometer-sized particles (1–100 nm in one dimension) is called nanofluid, some of the nanofluids used such as Cu water, CuO water, Al_2O_3 water, CuO-ethylene glycol, TiO_2 water, SiC water, MWCNT water, SWCNH water, Al_2O_3 synthetic oil, graphite water and silver water [12]. The experiment is conducted to find the performance of ETC using 0.3% TiO_2 nanofluid 30–50 nm average-sized particle, thermal conductivity increases as compared to its base fluid. It enhances the fluid properties and increases the heat transfer rate, he also compared efficiency, temperature rise for TiO_2 based nanofluid with its base fluid and showed that efficiency of ETC increased by 16.67% and temperature rises by 19% at the exit of the collector [75].

All-glass passive ETC is investigated and the result shows the efficiency is increased by 25.6% by using Al_2O_3 /DW instead of water as the working fluid in natural circulation and the maximum collector efficiency is 58.65% for mass flow of 60 L/h (0.06 vol%) [76]. The single-ended tube is studied numerically for natural convection heat transfer and fluid flow and the result showed that the overall Nusselt number increases with an increase in heat input and this effect is higher with an increase in the solid concentration of particle of size 100 nm in copper-water nanofluid, he also showed the effect of heat input, presence of nanoparticle and inclination angle on buoyancy force [77]. Three mass flow rate is experimented for calculating the efficiency of ETC with water and single-walled carbon nanotube nanofluid, he showed on a cloudy day using 0.2 vol% and mass flow rate of 0.025 kg/s for single-walled carbon nanotube the efficiency is 56.81%, he suggested that this type of collector is suitable for a cloudy day [78].

By using CuO nanofluid the performance and operating temperature are increased as compared to pure water, he investigated that the difference in temperature at lower volume concentration is higher as compared to higher volume concentration because of settling down of nanoparticle at high volume concentration and radiation absorption by the upper layer of nanofluid [55]. Graphene nanoplatelets are used as an absorbing medium for higher outlet temperature, the effect of different concentration and volumetric flow rate on efficiency and thermal performance of ETC is calculated, the efficiency is increased by 35.8% by using graphene nanoplatelets nanofluid for the flow rate of 1.5 l/min as compared to distilled water as a working fluid [79]. The selection of nanofluid (Ag with distilled water/ ZrO_2 with distilled water) is an important factor to improve the performance of evacuated tube solar collector, particle size, thermal conductivity, volume fraction of nanoparticle, mass flow rate is responsible for the overall performance of evacuated tube solar collector, he also observed that collector efficiency is higher for Ag (30 nm) as compared to ZrO_2 (50 nm) [80]. For different working fluids (water, Al_2O_3 /distilled water (0.03% and 0.06%)) and at a different time interval, the temperature difference is higher for Al_2O_3 compared to water under thermosiphon circulation inside ETC. The average tank temperature is maximum during a low mass flow rate for Al_2O_3 (0.06 vol%) [71].

Enclosed-type evacuated U-tube solar collector is investigated and found that density and thermal conductivity increases, specific heat decreases when volume concentration of nanoparticle increases from 0% to 1%; air, water and MWCNT/water nanofluid is used between absorber tube and U-tube to compare the conductance and found that using water the solar collector efficiency increases by 4% as compared to air and using MWCNT/water nanofluid heat transfer coefficient increase by 8% as compared to water, high thermal conductivity between copper fin and absorber tube increases the efficiency [81]. Table 2 represents the summary of the performance of the evacuated tube desalination system containing nanofluid.

6. Other types of solar still integrated with ETC/heat-pipe

The rate of production (0.48 L/h) is higher for 150 mL of water in the basin compared to other levels of 100 and 200 mL when ethanol filled heat pipe is inserted inside a twin-glass evacuated tube collector [29]. Comparison is done experimentally for standard (no PCM) and dual-PCM system, five tubes filled with tritriacontane (72°C) and five tubes filled with erythritol (118°C) and showed that water can be kept at high temperature for longer period of time when sunlight is not available, the efficiency of SWH system is increased by 26% [82].

Wick solar still (single-layered lined and plane wick) is compared with conventional solar still and showed that operating temperature, distillate output is higher for single-layered line wick and solar wick still have higher efficiency than basin-type solar still [61]. The efficiency is increased by increasing conductance between absorber tube and copper fin and decrease with increase in temperature of working fluid due to thermal losses, the performance of collector increases with decrease in air thermal resistance between U-tube and absorber tube [39].

Antifreeze (mixture of ethylene glycol and water) between copper tubes and absorber acts as a liquid fin. A three-dimensional analytical model is developed to study the thermal performance of co-axial conduits in all-glass vacuum tubes in which the absorber surface exhibit relatively higher temperature [83]. A co-axial conduit is inserted inside the absorber and the gap between the conduit and collector is filled by anti-freeze material, in the one-dimensional model he studied heat transfer and temperature variation [25]. The experiment is conducted using double basin solar still coupled with fourteen vacuum tubes at an inclination of 35° with and without black granite gravel and found that daily distillate yield is increased by 65% and 56% respectively [84]. The thermal performance is evaluated for solar water heating system using heat pipe evacuated tube collector which transmits heat quickly to solar fluid and found more efficient than flat plate [85].

7. Thermal modeling

7.1. Series connected evacuated tube collector

The detailed analysis for series-connected evacuated tube collector in which outlet of first ETC is connected

Table 2
Recent investigations showing the performance of integrated system loaded with nanofluid

Author(s)	Year/Investigation	Type of ETC/ number	Type (size)	Research findings
Mahendran et al. [75]	2012/Experimental	ETC/16 (forced)	TiO ₂ /water (30–50 nm)	Maximum efficiency of the system using nanofluid is 20% more than the system with distilled water, enhancement in heat transfer rate from absorber plate to working fluid
Sabiha et al. [78]	2015/Experimental	Heat pipe ETSC/12	Single walled carbon nano- tube	Maximum efficiency of the system is 93.43%, thermal performance is better, the efficiency of the collector with nanofluid on cloudy days is better than the efficiency of the collector with water on sunny days, efficient conversion of solar energy into thermal energy
Hussain et al. [80]	2015/Experimental	ETC/20 (forced)	Ag (30 nm) and ZrO ₂	Solar collector operates at higher temperature; collector efficiency for silver is more than zirconium oxide and heat loss from the collector is less
Ghaderian et al. [55]	2017/Experimental	ETC/18 (ther- mosyphon)	CuO/distilled water	Efficiency of the system is 51.4% with 0.06% of CuO with a higher mass flow rate, heat transfer rate and conductance increases
Zhiqiang et al. [59]	2017/Experimental	ETSC/18 (thermosy- phon)	Aluminium oxide (40 nm)	Efficiency of collector is 57.63% for 0.06 vol% with higher mass, the efficiency of collector increases with the use of nanofluid of higher thermal conductance, performance degrades at a higher volume concentration

to the inlet of second ETC and so on. The energy balance equation for ETC carrying Fluid which is used for calculating outlet temperature and useful energy for N-ETC is given in Eqs. (30)–(31). The expression for calculating outlet temperature and useful energy from N-ETC is given in Eqs. (32)–(35).

Rate of solar radiation available on ETC = Rate of thermal energy transferred from the blackened plate to the fluid + rate of thermal energy loss from the plate to ambient through the glass.

$$\alpha\tau^2 I(t)(2Rdx) = [F'h_{pt}(T_p - T_f) + U_{t,pa}(T_p - T_a)]2Rdx \quad (30)$$

Rate of thermal energy carried away by the flowing fluid = Rate of available energy to the fluid.

$$\dot{m}_f C_f \frac{dT_f}{dx} dx = F'h_{pt}(T_p - T_f)2\pi r dx \quad (31)$$

Using Eqs. (30) and (31) and applying boundary condition, the outlet temperature from the first collector is obtained as:

$$T_{fo1} = \left[\frac{PF_1 \alpha \tau^2 I(t)}{U_L} + T_a \right] \left[1 - \exp\left(-\frac{2\pi r L' U_L}{\dot{m}_f C_f}\right) \right] + T_{fi} \exp\left(-\frac{2\pi r L' U_L}{\dot{m}_f C_f}\right) \quad (32)$$

Similarly, outlet temperature from Nth collector can be obtained as:

$$T_{foN} = \frac{(AF_R \alpha \tau)_1 (1 - K_k^N)}{\dot{m}_f C_f (1 - K_k)} I(t) + \frac{(A_R F_R U_L)_1}{\dot{m}_f C_f} \times \frac{(1 - K_k^N)}{(1 - K_k)} T_a + K_k^N T_{fi} \quad (33)$$

where $K_k = 1 - \frac{A_R F_R U_L}{\dot{m}_f C_f}$ and N = number of evacuated tube collectors.

The rate of useful thermal energy gain from N-ETC is given as:

$$\dot{Q}_{uN} = \frac{(1 - K_k^N)}{(1 - K_k)} (AF_R (\alpha \tau))_1 I(t) + \frac{(1 - K_k^N)}{(1 - K_k)} (AF_R U_L)_1 (T_{fi} - T_a) \quad (34)$$

Or,

$$\dot{Q}_{uN} = (\alpha \tau)_{\text{eff}} I(t) - (UA)_{\text{eff}} (T_{fi} - T_a) \quad (35)$$

Eq. (35) gives the useful energy gain for the N series-connected evacuated tubular collector [86]. Various unknown terms are used in Eqs. (30)–(33) are given in Appendix-A.

7.2. Series connected evacuated tube in combination with single slope still

The thermal modeling and incorporated characteristic equation for series-connected N identical evacuated

tubular collector integrated single slope solar still (N-ETC-SS). The schematic diagram of this series connected N-ETC-SS is given in Fig. 10.

The energy balance equation of various components of active single slope solar still used is given in Eqs. (36)–(39) [87].

7.2.1. Inner surface of the glass cover

$$\alpha'_g I_s(t) A_g + h_{1w} (T_w - T_{gi}) A_b = \frac{K_g}{L_g} (T_{gi} - T_{go}) A_g \tag{36}$$

where $\alpha'_g = (1 - R_g)\alpha_g$ represents the fraction of solar flux absorbed by the glass cover and $h_{1w} = h_{rwg} + h_{cwg} + h_{swg}$ represents the rate of total heat transfer coefficient from the water surface to the inner surface of the glass cover.

7.2.2. Outer surface of glass cover

$$\frac{K_g}{L_g} (T_{gi} - T_{go}) A_g = h_{1g} (T_{go} - T_a) A_g \tag{37}$$

where $h_{1g} = h_{rg} + h_{cg}$ or $h_{1g} = 5.7 + 3.8 V$.

7.2.3. Water mass in basin

$$\dot{Q}_{uN} + \alpha'_w I_s(t) A_b + h_{bw} (T_b - T_w) A_b = h_{1w} (T_w - T_{gi}) A_b + M_w C_w \frac{dT_w}{dt} \tag{38}$$

where $\alpha'_w = (1 - R_g)(1 - \alpha_g)(1 - R_w)\alpha_w$ equivalent to the fraction of solar flux absorbed by water mass and \dot{Q}_{uN} is the rate of useful thermal output from N identical ETC connected in series.

7.2.4. Basin liner

$$\alpha'_b I_s(t) A_b = h_{bw} (T_b - T_w) A_b + h_{ba} (T_b - T_a) A_b \tag{39}$$

where $\alpha'_b = (1 - R_g)(1 - \alpha_g)(1 - R_w)(1 - \alpha_w)\alpha_b$ is the fraction of solar flux absorbed by basin liner.

Using Eqs. (35)–(39), one can get the first-order differential equation of water temperature (T_w for N-ETC-SS as follows:

$$\frac{dT_w}{dt} + a_1 T_w = f_1(t) \tag{40}$$

The expression for a_1 and $f_1(t)$ used in Eq. (40) and various unknown terms used in Eqs. (36)–(39) are given in Appendix-A.

The solution of differential Eq. (40) can be inscribed as:

$$T_w = \frac{\bar{f}_1(t)}{a_1} (1 - e^{-a_1 t}) + T_{w0} e^{-a_1 t} \tag{41}$$

where T_{w0} is the temperature of water at $t = 0$ and $\bar{f}_1(t)$ is the average value of $f_1(t)$ during the time interval 0 to t .

After computing the value of T_w with the help of Eq. (41), values of glass temperature (T_{gi} and T_{go}) can be evaluated by using Eqs. (36) and (37) as follows.

$$T_{gi} = \frac{\alpha'_g I_s(t) A_g + h_{1w} T_w A_b + U_{c,ga} T_a A_g}{U_{c,ga} A_g + h_{1w} A_b} \tag{42}$$

$$T_{go} = \frac{\frac{K_g}{L_g} T_{gi} + h_{1g} T_a}{\frac{K_g}{L_g} + h_{1g}} \tag{43}$$

The hourly production of potable water (\dot{m}_{ew}) from N-ETC-SS can be computed as follows:

$$\dot{m}_{ew} = \frac{h_{ewg} A_b (T_w - T_{gi})}{L} \times 3,600 \tag{44}$$

where L can be defined as the amount of thermal energy required to evaporate the unit mass of water (latent heat).

The hourly and daily exergy gain of the N-ETC-SS system can be calculated as:

$$\dot{G}_{ex} = h_{ewg} A_b \left[(T_w - T_{gi}) - (T_a + 273) \ln \left\{ \frac{(T_w + 273)}{(T_{gi} + 273)} \right\} \right] \tag{45}$$

$$G_{ex} = \sum_{t=1}^{t=24} \left[h_{ewg} A_b \left[(T_w - T_{gi}) - (T_a + 273) \ln \left\{ \frac{(T_w + 273)}{(T_{gi} + 273)} \right\} \right] \right] \tag{46}$$

The hourly and daily energy gain of N-ETC-SS system can be expressed as:

$$\dot{E} = \frac{(\dot{m}_{ew} \times L)}{3,600} \tag{47}$$

$$E = \frac{\sum_{t=1}^{t=24} [\dot{m}_{ew} \times L]}{3,600} \tag{48}$$

The hourly and daily exergy efficiency N-ETC-SS system can be expressed as:

$$\eta_{\text{hourly,ex}} = \frac{\dot{G}_{ex}}{\dot{E}x_c(t) + [0.933 \times A_b \times I_s(t)] + P_u} \times 100 \tag{49}$$

$$\eta_{\text{daily,ex}} = \frac{G_{ex}}{\sum_{t=1}^{10} [\dot{E}x_c(t) + [0.933 \times A_b \times I_s(t)] + P_u]} \times 100 \tag{50}$$

where

$$\dot{E}x_c(t) = (\dot{m}_f \times C_f) \left[(T_{ioN} - T_{fi}) - (T_a + 273) \times \ln \left(\frac{T_{ioN} + 273}{T_{fi} + 273} \right) \right] \tag{51}$$

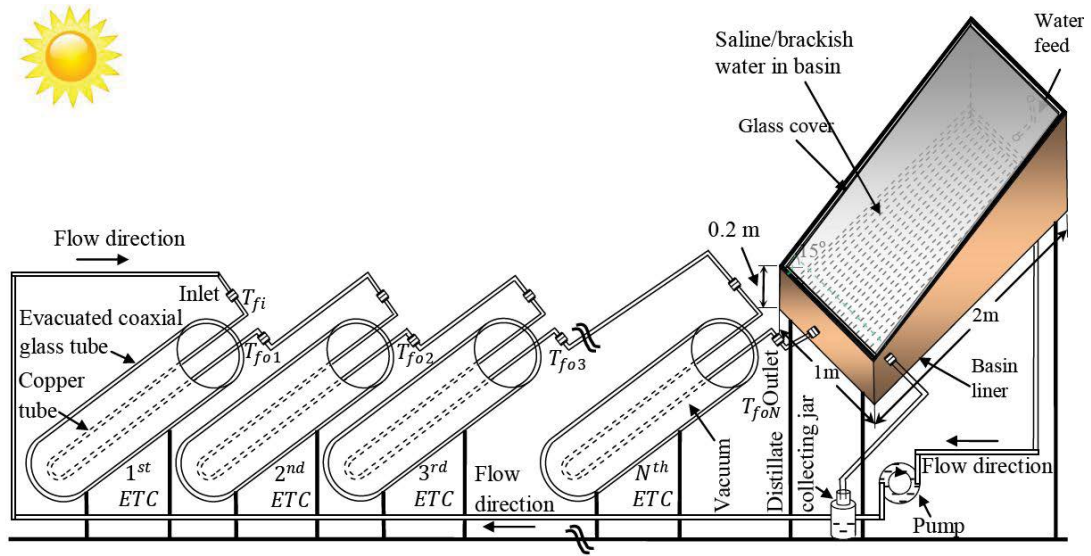


Fig. 10. Schematic diagram of the single-slope solar still incorporated with N identical ETC connected in series (N-ETC-SS) adapted from the study of Singh and Tiwari [87].

The hourly and daily energy efficiency of the N-ETC-SS system can be expressed as:

$$\eta_{\text{hourly, en}} = \frac{\dot{E}}{\left[\dot{Q}_{uN}(t) + A_b I_s(t) + \frac{P_u}{0.38} \right]} \times 100 \quad (52)$$

$$\eta_{\text{daily, en}} = \frac{E}{\sum_{t=1}^{24} \left[\dot{Q}_{uN}(t) + A_b I_s(t) + \frac{P_u}{0.38} \right]} \times 100 \quad (53)$$

The hourly production of potable water, exergy and energy gain, exergy and energy efficiency for series-connected N-ETC-SS can be easily obtained by using the above equations [87].

7.3. Series connected evacuated tube collector double slope still

The schematic diagram of series-connected N-ETC-DS is given in Fig. 11. Energy balance equation for various components of active double slope solar still can be inscribed as shown below, double slope still contains east and west glass cover and the energy balance equation for the inner and outer face of both the glass cover is written in Eqs. (54)–(57) [87].

For inner surface of east glass cover:

$$\alpha'_s I_{SE}(t) A_{gE} + h_{1wE} (T_w - T_{giE}) \frac{A_b}{2} - h_{EW} (T_{giE} - T_{giW}) A_{gE} = \frac{K_g}{L_g} (T_{giE} - T_{goE}) A_{gE} \quad (54)$$

For outer surface of east glass cover:

$$\frac{K_g}{L_g} (T_{giE} - T_{goE}) A_{gE} = h_{1gE} (T_{goE} - T_a) A_{gE} \quad (55)$$

For inner surface of west glass cover:

$$\alpha'_s I_{SW}(t) A_{gW} + h_{1wW} (T_w - T_{giW}) \frac{A_b}{2} + h_{EW} (T_{giE} - T_{giW}) A_{gE} = \frac{K_g}{L_g} (T_{giW} - T_{goW}) A_{gW} \quad (56)$$

For outer surface of west glass cover:

$$\frac{K_g}{L_g} (T_{giW} - T_{goW}) A_{gW} = h_{1gW} (T_{goW} - T_a) A_{gW} \quad (57)$$

For basin liner:

$$\alpha'_b (I_{SE}(t) + I_{SW}(t)) \frac{A_b}{2} = h_{bw} (T_b - T_w) A_b + h_{ba} (T_b - T_a) A_b \quad (58)$$

For water mass in basin:

$$(M_w C_w) \frac{dT_w}{dt} = (I_{SE}(t) + I_{SW}(t)) \alpha'_w \frac{A_b}{2} + h_{bw} (T_b - T_w) A_b - h_{1w} (T_w - T_{giE}) \frac{A_b}{2} - h_{1w} (T_w - T_{giW}) \frac{A_b}{2} + \dot{Q}_{uN} \quad (59)$$

Using Eq. (34) and Eqs. (54)–(59), one can get the first-order differential equation of water temperature (T_w for N-ETC-DS as follows [87].

$$\frac{dT_w}{dt} + a_1 T_w = f_1(t) \quad (60)$$

The expression for a_1 and $f_1(t)$ used in Eq. (60) and various unknown terms used in Eqs. (54)–(59) are given in Appendix-A. The solution of differential Eq. (60) can be inscribed as:

$$T_w = \frac{\bar{f}_1(t)}{a_1} (1 - e^{-a_1 t}) + T_{w0} e^{-a_1 t} \quad (61)$$

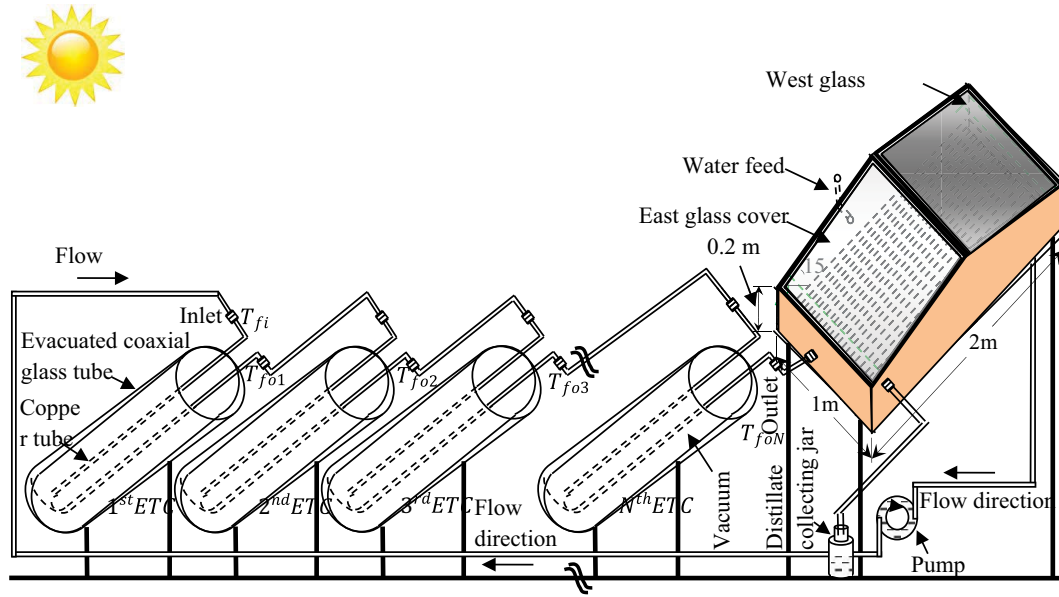


Fig. 11. Schematic diagram of the double slope solar still incorporated with N identical ETC connected in series (N-ETC-DS) adapted from the study of Singh and Tiwari [87].

where T_{w0} is the temperature of water at $t = 0$ and $\bar{f}_1(t)$ is the average value of $f_1(t)$ during the time interval 0 to t . After computing the value of T_w with the help of Eq. (61), values of different glass temperatures (T_{giE} , T_{giW} , T_{goE} and T_{goW}) can be evaluated using Eqs. (54) and (55) as follows.

$$T_{giE} = \frac{A_1 + A_2 T_w}{P} \tag{62}$$

$$T_{giW} = \frac{B_1 + B_2 T_w}{P} \tag{63}$$

$$T_{goE} = \frac{\frac{K_g}{L_g} T_{giE} + h_{1gE} T_a}{\frac{K_g}{L_g} + h_{1gE}} \tag{64}$$

$$T_{goW} = \frac{\frac{K_g}{L_g} T_{giW} + h_{1gW} T_a}{\frac{K_g}{L_g} + h_{1gW}} \tag{65}$$

where expressions of unknown terms are used in Eqs. (62)–(65) are given in Appendix-A [89]. After computing the value of water temperature (T_w) and glass temperature (T_{giE} and T_{giW}), the hourly production of potable water (\dot{m}_{ew}) can be computed as follows.

$$\dot{m}_{ew} = \frac{h_{ewgE} \frac{A_b}{2} (T_w - T_{giE}) + h_{ewgW} \frac{A_b}{2} (T_w - T_{giW})}{L} \times 3,600 \tag{66}$$

where L stands for the amount of thermal energy required to evaporate the unit mass of water (latent heat) as reported by Fernández & Chargoy [88] and Toyama and Kangkuv [89].

Following Nag [90], hourly and daily exergy gain of the proposed system can be inscribed as:

$$\dot{G}_{ex} = h_{ewgE} \frac{A_b}{2} \left[(T_w - T_{giE}) - (T_a + 273) \ln \left\{ \frac{(T_w + 273)}{(T_{giE} + 273)} \right\} \right] + h_{ewgW} \frac{A_b}{2} \left[(T_w - T_{giW}) - (T_a + 273) \ln \left\{ \frac{(T_w + 273)}{(T_{giW} + 273)} \right\} \right] \tag{67}$$

where \dot{G}_{ex} represents hourly exergy gain for the proposed system, h_{ewgE} represents evaporative heat transfer coefficient from the water surface to inner surface of the east glass cover, h_{ewgW} represents evaporative heat transfer coefficient from the water surface to inner surface of west glass cover:

$$G_{ex} = \sum_{t=1}^{t=24} \dot{G}_{ex} \tag{68}$$

Here, G_{ex} represents daily exergy gain for the proposed system.

Following Tiwari [4], hourly and daily energy gain of the proposed system can be written as:

$$\dot{E} = \frac{(\dot{m}_{ew} \times L)}{3,600} \tag{69}$$

$$E = \frac{\sum_{t=1}^{t=24} [\dot{m}_{ew} \times L]}{3,600} \tag{70}$$

where \dot{m}_{ew} is hourly production of potable water and L is latent heat, \dot{E} hourly energy gain and E is daily energy gain.

The hourly and daily exergy efficiency for the N-ETC-DS system can be calculated by using the expression reported by Singh & Tiwari [91] and Singh et al. [92] respectively and is inscribed as:

$$\eta_{\text{hourly,ex}} = \frac{\dot{G}_{\text{ex}}}{\dot{E}x_c(t) + \left[0.933 \times \frac{A_b}{2} \times (I_{\text{SE}}(t) + I_{\text{SW}}(t)) \right] + P_u} \times 100 \tag{71}$$

$$\eta_{\text{daily,ex}} = \frac{G_{\text{ex}}}{\sum_{t=1}^{10} \left[\dot{E}x_c(t) + \left[0.933 \times \frac{A_b}{2} \times (I_{\text{SE}}(t) + I_{\text{SW}}(t)) \right] + P_u \right]} \times 100 \tag{72}$$

$$\dot{E}x_c(t) = \left(\dot{m}_f \times C_f \right) \left[(T_{\text{foN}} - T_{\text{fi}}) - (T_a + 273) \times \ln \left(\frac{T_{\text{foN}} + 273}{T_{\text{fi}} + 273} \right) \right] \tag{73}$$

The hourly and daily energy efficiency for the N-ETC-DS system can be inscribed as:

$$\eta_{\text{hourly,en}} = \frac{\dot{E}}{\left[\dot{Q}_{uN}(t) + \frac{A_b}{2} (I_{\text{SE}}(t) + I_{\text{SW}}(t)) + \frac{P_u}{0.38} \right]} \times 100 \tag{74}$$

$$\eta_{\text{daily,en}} = \frac{E}{\sum_{t=1}^{10} \left[\dot{Q}_{uN}(t) + \frac{A_b}{2} (I_{\text{SE}}(t) + I_{\text{SW}}(t)) + \frac{P_u}{0.38} \right]} \times 100 \tag{75}$$

where \dot{E} is hourly energy output from the system, $\dot{Q}_{uN}(t)$ is the rate of useful thermal output from N identical ETC connected in series.

$\dot{Q}_{uN}(t)$ can be calculated by the expression in which value T_{fi} is equal to T_w as collectors form a closed loop with basin [93].

8. Comparison and discussion

Fig. 12 shows energy and exergy values for different evacuated tube integrated systems. The system N-ETC-SS is having the highest energy and second-highest exergy efficiency as compared to other systems because the temperature attained in series connected evacuated tube collector is higher as compared to a parallel connection. The exergy gain for N-ETC-SS is lower as compared to N-PVT-CPC-SS because the optimum value of mass flow rate is reduced for N-ETC-SS. The exergy efficiency is 87.13% and 86.21% higher for N-PVT-CPC-SS and N-ETC-SS as compared to the exergy efficiency of the EISS forced system in winter because of lower exergy input. The exergy is 82.66% and 81.42% higher for N-PVT-CPC-SS and N-ETC-SS as compared to the EISS system in summer because the EISS system is connected in parallel gives lower water temperature. The energy efficiency of N-ETC-SS is 23.61% higher compared to the N-PVT-CPC-SS system because the energy required to produce potable water is reduced or efficient utilization by N-ETC-SS.

Fig. 13 shows the cost per liter (CPL) of water yielded from various systems. The minimum cost of potable water is for the ETC-HP (HP – heat pipe) system because the daily rate of production is higher when the condenser of the heat pipe is in direct contact with the basin water which provides a better heat transfer rate. The cost per litre for EISS – forced system, ETC-DLSW and ETC-SSW (DLSW – double layered

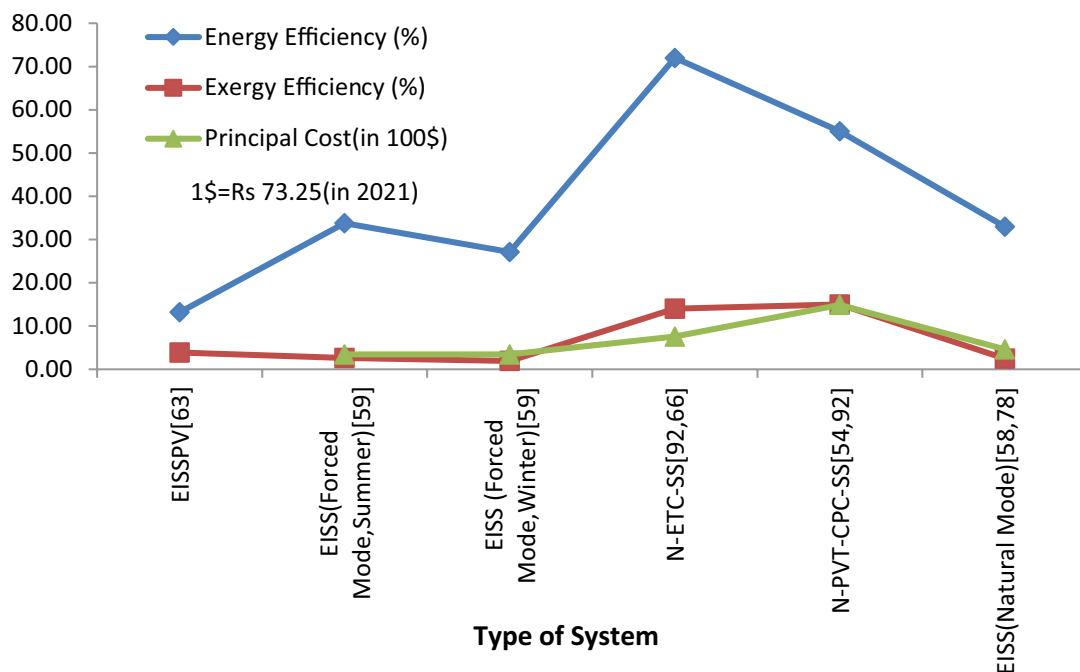


Fig. 12. Energy and exergy efficiency variation in a different system.

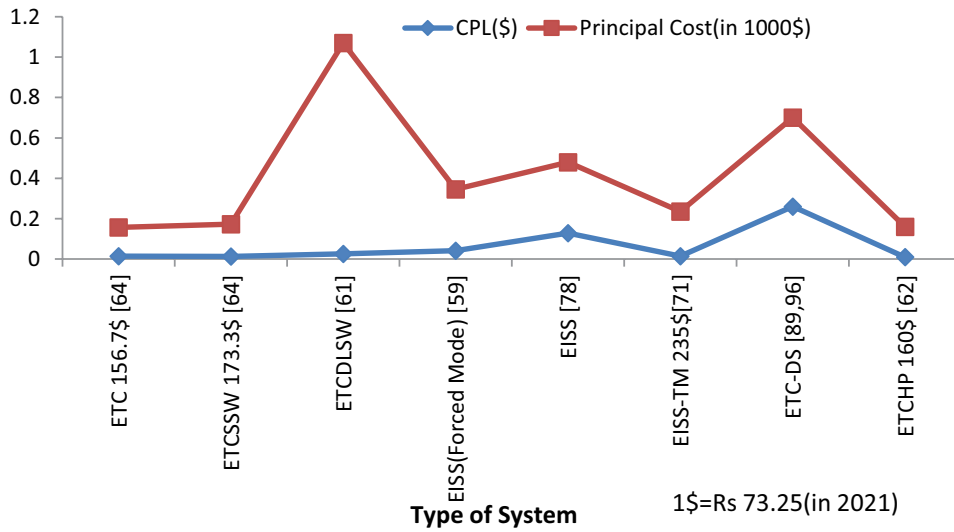


Fig. 13. Variation in cost per liter (CPL) for different desalination systems.

squared wick; SSW – stainless steel wool) system is lower because the evaporation rate is higher for this system when compared to EISS in natural mode.

Fig. 14 gives the comparison between daily maximum potable water yields for different evacuated tube collector integrated distillation units. The daily yield is 76.21% and 74.38% higher for N-PVT-CPC-SS and N-ETC-SS as compared to the EISS system having 24 tubes connected in parallel. The concentration of beam radiation on the parabolic surface on the receiver in the case of N-PVT-CPC-SS gives a higher yield. The maximum daily yield for EISS-PV and ETC-SSW is 4.84% and 28.10% lower respectively than the EISS-TM system in which forced convection is generated results in an increase in yield and hourly efficiency. In the case of the ETC-SSW system overall thermal conductivity increases by the use of stainless-steel wool and results in enhancement in heat transfer rate.

Fig. 15 indicates the difference between basin water and cover temperature for various systems. The difference is higher for EISS [27] in June for Indian climatic conditions followed by N-ETC-SS and lowers for EISS-PV and ETC-HP systems. The basin water temperature is highest for EISS in forced mode; heat transfer is more in forced circulation and lowest for ETC-HP in which natural circulation heat pipes are used. The module temperature of EISS-PV is higher when compared to other cases. The difference is higher in the case of EISS (forced mode) and N-ETC-SS because of the higher temperature of basin water and is lower for the ETC-PV system. The latter system runs in natural mode and PV module temperature is higher, increasing the number of tubes in the ETC-PV system, the yield difference decreases between glass and PV module cover.

Fig. 16 shows how hourly yield varies with depth for a different integrated system. In the case of EISS with a depth

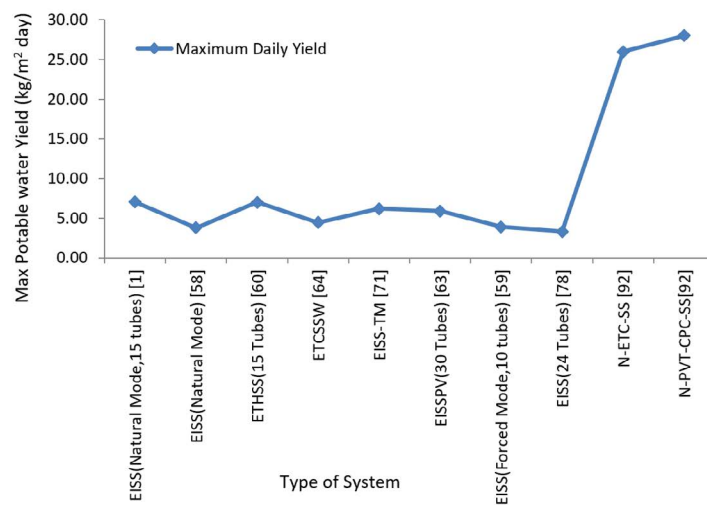


Fig. 14. Daily maximum potable water yield from various integrated systems.

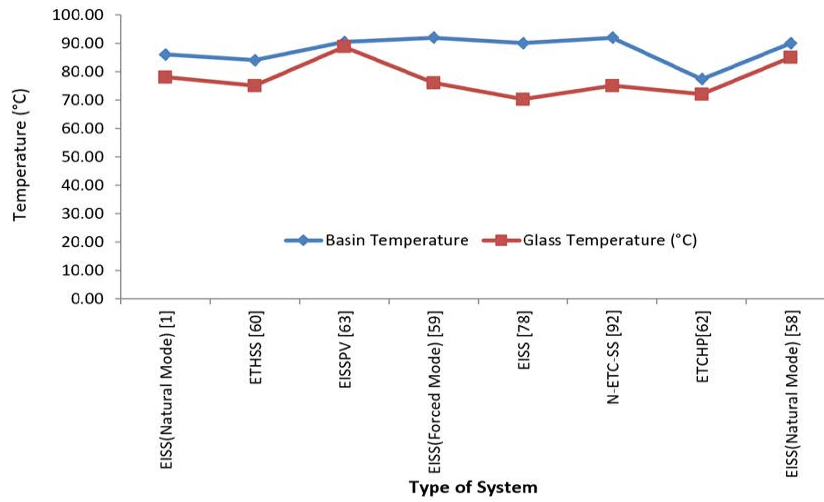


Fig. 15. Difference between the basin and cover temperature of still for various systems.

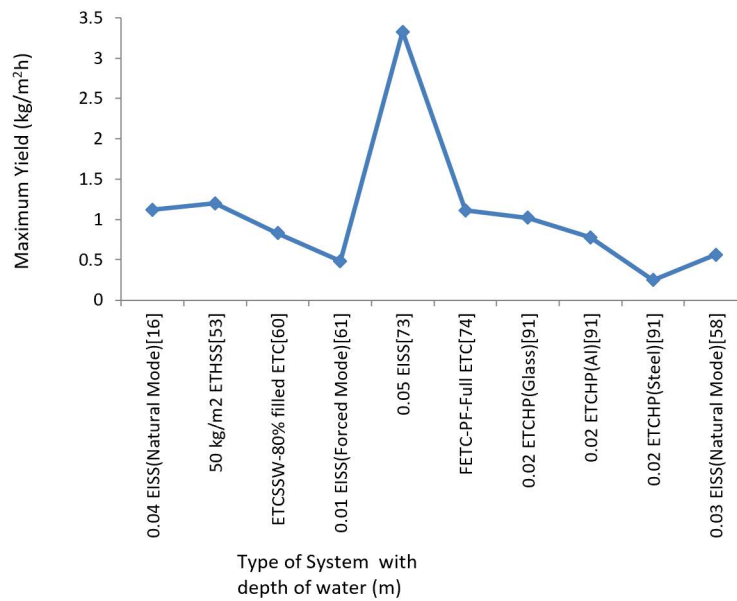


Fig. 16. Variation of hourly maximum yield with respect to depth inside various systems.

of 0.05 m yield is higher the number of evacuated tubes used in this case is 24. Yield also depends on the surface area of condensation and the number of evacuated tubes/heat pipes used. Yield is lower for lower depth (0.01 m) and it increases with an increase in depth (0.05 m) of water but yield becomes lower when depth is further increased. Different cover material still gave different yield; glass cover yield is higher as compared to other metal cover material.

Fig. 17 illustrates the system efficiency of the integrated system; the ETC-WS system showed the highest efficiency, in this evaporation rate is higher followed by FETC-PF and ETC-SSW respectively. The lowest efficiency is achieved for the ETC-HP system with steel as a cover material because the solar gain from the cover material

is less in spite of higher thermal conductivity. The DLSW still showed improved efficiency because of the higher evaporation rate as compared to other systems.

Fig. 18 gives the idea of the annual yield of potable water for various systems in which wick still performs better as compared to others because the wetted wick due to capillary action enhances the rate of evaporation. Full-ETC with propeller fan gave the highest yield because the evaporate water from the evacuated tube goes to the condensation chamber where turbulence is generated by propeller fan after ETC-HP system in which natural circulation is used. The heat pipe system gave a lesser yield than the wick still integrated system. The annual yield of the ETC-WS system is 86.32% and 44.12% higher than EISS (forced) and ETC-HP

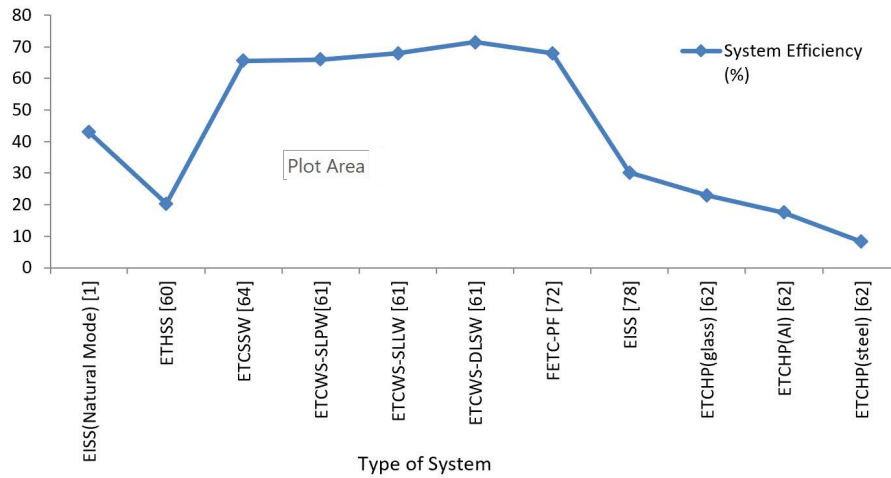


Fig. 17. Variation in system efficiency for different evacuated tube collector-still systems.

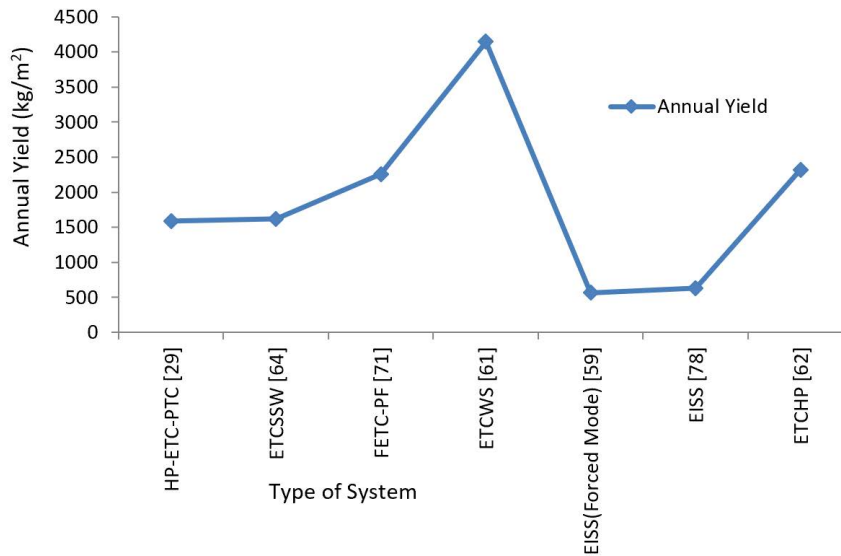


Fig. 18. Comparison of a different system based on annual yield.

system respectively. In the ETC-HP system condenser of heat, pipe is in direct contact with basin water but in the case of EISS (forced), the rate of convection losses is higher.

9. Economic analysis of ETC integrated distillation unit

Capital cost, interest rate, maintenance cost, operating cost and subsidy gives the payback period for the solar still. Various method used for economic analysis, capital recovery factor $S = P(1 + i)^n$, uniform annual cost $R = P\{i(1 + i)^n / [(1 + i)^n - 1]\}$ and sinking fund factor $S = R\{[(1 + i)^n - 1] / i\}$, where S = future value, P = present value, i = interest rate, n = number of year, R = uniform annual cost [4].

A large surface area is required for obtaining maximum yield and CSS is not economical due to its low productivity [14]. A simple payback period is used and net present value to evaluate the economic value of the project, evacuated tube collector is more expensive than flat plate collector for small scale water heating purpose, annual operation and

maintenance cost is 1% of initial capital cost. The distilled water annual cost in terms of kWh and kg is \$0.198 per kWh and \$0.128 per kg [19]. Utilizing nanofluid in the solar system improves the system performance by reducing the thermal resistance [50]. The detailed comparison of a cost analysis of various systems is tabulated in Table 3.

10. ETC integrated desalination unit challenges

Evacuated tube dimension, the center distance between two tubes and shadow effect varies the optical efficiency of the evacuated tube throughout the day. Fragility (annealed borosilicate glass), overheating, pressure, cost and maintenance are the points to be considered while using an evacuated tube [22].

Effectiveness in heat transfer between absorber tube due to radiation and U-tube containing heat transfer fluid has to be increased by minimizing heat loss. Distance and insulation between outlets of ETC which is connected to

Table 3
Economic analysis of various desalination systems integrated with evacuated tube/heat-pipe

Parameters	Type of system/(Unit)	Heat pipe with solar still Shafii et al. [8]	ETC (heat pipe) and parabolic trough Shafii et al. [29]	ETC integrated solar still Zhiqiang et al. [59]	ETC integrate still and thermoelectric module Shafii et al. [65]	ETC (heat pipe) integrated still Shafii et al. [63]
Principal cost	(\$)	35.3	568	694.96	235	160
Salvage value (10% of principal value)	(\$)	3.53	56.8	104.26	23.5	16
Life	(y)	20	20	15	20	20
Interest rate	(%)	10	10	12	10	10
Capital recovery factor	–	0.117	0.117	0.15	0.117	0.117
Sink fund factor	–	0.0175	0.175	0.03	0.0175	0.0175
Annual first cost	(\$)	15.9	66.72	104.26	27.495	18.8
Annual salvage value	(\$)	0.06	0.992	20.83	0.399	0.28
Annual maintenance cost	(\$)	0.615	10.01	15.63	4.124	2.82
Annual cost per m ²	(\$)	4.655	75.73	116.72	31.219	21.34
Average daily yield	(kg/m ²)	1.976	4.03	2.5	6.186	6.350
Annual yield of the still	(kg/m ²)	721.25	1,587.7	912.5	2,257.8	2,317.8
Annual useful energy (annual yield × latent heat of vaporization)	kWh	468.8	1,030.7	593.1	1,467.6	1,506.5
Annual cost of distilled water per kg (annual first cost/annual yield)	(\$)	0.0057	0.0421	0.128	0.0122	0.0081
Annual cost of distilled water per kWh (annual first cost/useful energy)	(\$)	0.0087	0.0647	0.198	0.0187	0.0125
CPL per unit area of still	(\$)	0.0064	0.0478	0.1279	0.0138	0.0092

the inlet of still should be analyzed to reduce availability loss. Exergy loss is higher at high temperatures so while using the evacuated tube in series, the still should be properly designed and optimized to give a higher yield. Finally, the still integrated ETC should be designed in such a way that it gives a good yield, minimum payback period, maintenance-free and it becomes an independent freshwater supply system without any complexity.

11. Conclusion

Various research findings such as maximum yield, water temperature, glass cover temperatures, the efficiency of the combined system are shown with the help of which system can be optimized. Thermal modeling for the series-connected combined system is shown from which hourly and daily energy gain, hourly and daily exergy gain, hourly and daily energy efficiency and hourly and daily exergy efficiency can be evaluated. The following conclusions have been made on the basis of the present review:

- The output of active solar still depends on natural and forced circulation, depth of water in still, solar intensity, inclination angle, number of evacuated tubes are used, heat storage materials used, the temperature of glass cover and its material and mass flow rate.
- Performance of the system is evaluated by various parameters like yield, efficiency, exergy, energy payback

time, energy production factor, life cycle conversion efficiency, exergoeconomic and enviroeconomic considerations. Yield is increased by optimizing evaporative and convective heat transfer coefficients for different depths.

- Utilization of heat storage material in an evacuated tube and in still reduces the size of the system. Using nanofluids better heat transfer rate can be achieved and the system performs better during cloudy days.
- Different combinations of evacuated tube/heat pipe still yielded a different result. The maximum hourly yield is for EISS and the annual yield is more for the ETC-WS system. Energy efficiency is higher for N-ETC-SS but exergy efficiency and maximum daily yield are higher for N-PVT-CPC-SS.
- Energy efficiency, exergy efficiency, system efficiency, daily, hourly and annual yield, basin and glass cover temperature is compared for various systems. Hence there is a requirement for an optimized design for maximum productivity.

Symbols

A	–	Area, m ²
A_a	–	Aperture area of solar collector, m ²
A_b	–	Area of the basin, m ²
A_c	–	Surface area of collector, m ²
A_c	–	Diameter of inner glass tube × total length of tubes, m ²

A_s	–	Basin liner still area, m ²	L_g	–	Thickness of glass cover, m
A_w	–	Area of water surface, m ²	L_v	–	Characteristic dimension of condensing cover, m
A_g	–	Area of the glass cover, m ²	l	–	Gap width, m
α_1	–	Thermal diffusivity	L'	–	Length, m
C_p	–	Specific heat at constant pressure, J/Kg°C	\dot{m}_f	–	Mass flow rate of fluid/water, kg/s
C_f	–	Specific heat capacity, J/kg K	\dot{m}_{ew}	–	Mass of distillate from single slope solar still, kg
d_1^f	–	Riser tube diameter, m	m_{ew}	–	Hourly distillate output, kg/m ²
d_2	–	Glass tube diameter, m	M_w	–	Mass of water in basin, kg
dx	–	Elemental length, m	PF_c	–	Penalty factor due to the glass covers for the glazed portion
\dot{E}	–	Hourly energy output, kWh	n	–	Unknown constant in Nusselt number expression
E	–	Daily energy output, kWh	PF_1	–	Penalty factor first, dimensionless
ϵ_r	–	Emissivity of the riser	PF_2	–	Penalty factor second, dimensionless
ϵ_g	–	Emissivity of the glass tube	PVT	–	Photovoltaic thermal
\dot{E}_x	–	Energy flux associated with the system	Pr	–	Prandtl number, dimensionless
$\dot{E}_{x_{sun}}$	–	Exergy input from the sun, W	P_w	–	Partial saturated vapor pressure at condensing cover temperature, N/m ²
F_R	–	Collector heat removal factor	P_u	–	Hourly pump work
FF	–	Fill factor, dimensionless	P_{ci}	–	Partial saturated vapor pressure at condensing cover temperature, N/m ²
F'	–	Collector efficiency factor, dimensionless	q_u	–	Useful energy associated with the system at temperature T
\dot{G}_{ex}	–	Hourly exergy gain, kWh	Q_L	–	Thermal loss, W
G_{ex}	–	Daily exergy gain, kWh	q_{ew}	–	Rate of evaporative heat transfer, W/m ²
g	–	Gravitational acceleration, m/s ²	Q_{uN}	–	Useful energy gain for N identical collector connected in series, kWh
Gr	–	Grashof number	R	–	Outer radius of the glass tube, m
G	–	Solar irradiation, W/m ²	r	–	Radius of U-shaped copper tube, m
h_{cw}	–	Convective heat transfer coefficient, W/m ² K	R_{o1}	–	Inner radius of an outer glass tube of the evacuated coaxial glass tube, m
h_{ew}	–	Evaporative heat transfer coefficient, W/m ² K	R_{i2}	–	Outer radius of an inner glass tube of the evacuated coaxial glass tube, m
h_{cwg}	–	Convective heat transfer coefficient from water to inner surface of the glass cover, W/m ² K	R_{o2}	–	Outer radius of an outer glass tube of the evacuated coaxial glass tube, m
h_{ewg}	–	Evaporative heat transfer coefficient from the water surface to the inner surface of the glass cover, W/m ² K	r'	–	Radius of copper tube in ETC
h_c	–	Convective heat transfer coefficient, W/m ² K	R'	–	Reflectivity
h_{ba}	–	Heat transfer coefficient from blackened surface to ambient, W/m ² K	T_{ioN}	–	Outlet water temperature at the end of N th water collector, °C
h_{bw}	–	Heat transfer coefficient from blackened surface to water mass, W/m ² K	T_{fi}	–	Temperature of the inlet of first ETC
h	–	Heat transfer coefficient, W/m ² K	T_{gi}	–	Glass temperature at the inner surface of the glass cover, °C
h_{rwg}	–	Radiative heat transfer coefficient from the water surface to the inner surface of the glass cover, W/m ² K	T_s	–	Inner glass tube temperature
h_r	–	Radiative heat transfer coefficient, W/m ² K	T_r	–	Riser tube temperature
h_{1w}	–	Total heat transfer coefficient from the water surface to the inner surface of the glass cover, W/m ² K	T	–	Time, s
h_{1ww}	–	Total heat transfer coefficient from the water surface to west glass cover	ΔT	–	Temperature difference across the cavity
h_{1g}	–	Total heat transfer coefficient from the water surface to inner glass cover, W/m ² K	T_{gi}	–	Glass cover temperature, K
$I_s(t)$	–	Solar radiation on the glass cover of a solar still, W/m ²	T_{go}	–	Temperature of the outer surface of the glass cover
$I_c(t)$	–	Intensity of solar radiation on evacuated tube collector, W/m ²	T	–	Temperature, K
$I(t)$	–	Solar intensity on collector, W/m ²	T_s	–	Sun temperature, K
k	–	Thermal conductivity, W/m K	T_{out}	–	Fluid outlet temperature, °C
K_g	–	Thermal conductivity of glass cover	T_{in}	–	Fluid inlet temperature, °C
K_v	–	Thermal conductivity of humid air, W/m ² °C	T_m	–	Mean temperature of heat transfer fluid, °C
l	–	Thickness, m	T^a	–	Ambient temperature, °C
l_1	–	Tube length, m	T_{ci}	–	Inner temperature of condensing cover, °C
L	–	Latent heat of vaporization of water, J/kg	T_w	–	Water temperature, °C
			T_{w0}	–	Water temperature at $t = 0$, °C
			U_L	–	Overall heat transfer coefficient

- $U_{t,pa}$ — Overall heat transfer coefficient from absorber plate to ambient through the glass cover, $W/m^2 K$
 V — Velocity of air, m/s

Greek

- α — Absorptivity (fraction)
 α'_b — Portion of solar energy absorbed by basin liner
 α'_g — Fraction of solar flux absorbed by a glass cover
 α'_w — Fraction of solar energy absorbed by water mass
 $(\alpha\tau)_{eff}$ — Product of effective absorptivity and transmissivity
 σ — Stefan–Boltzmann constant, $W/m^2 K^4$
 β — Coefficient of thermal expansion
 ε_i — Instant exergy efficiency
 η — Efficiency, %
 η_i — Instant energy efficiency
 η_{ei} — Instant energy efficiency for the combined system
 τ — Transmissivity
 ν — Kinematic viscosity

Subscript

- f — Fluid
 p — Plate
 E — East
 W — West

References

- [1] K. Sampathkumar, T.V. Arjunan, P. Senthilkumar, The experimental investigation of a solar still coupled with an evacuated tube collector, *Energy Sources Part A*, 35 (2013) 261–270.
- [2] G.N. Tiwari, L. Sahota, Review on the energy and economic efficiencies of passive and active solar distillation system, *Desalination*, 401 (2017) 151–179.
- [3] T. Arunkumar, R. Velraj, D.C. Denkenberger, R. Sathyamurthy, K. Vinoth Kumar, A. Ahsan, Productivity enhancements of compound parabolic concentrator tubular solar stills, *Renewable Energy*, 88 (2016) 391–400.
- [4] G.N. Tiwari, *Solar Energy: Fundamentals, Design, Modeling and Applications*, Narosa Publishing House, New Delhi, 2002.
- [5] S. Abdallah, O. Badran, M.M. Abu-Khader, Performance evaluation of a modified design of a single slope solar still, *Desalination*, 219 (2008) 222–230.
- [6] R. Sathyamurthy, S.A. El-Agouz, P.K. Nagarajan, J. Subramani, T. Arunkumar, D. Mageshbabu, B. Madhu, R. Bharathwaaj, N. Prakash, A review of integrating solar collectors to solar still, *Renewable Sustainable Energy Rev.*, 77 (2017) 1069–1097.
- [7] A. Kumar, S. Kumar, U. Nagar, A. Yadav, Experimental study of thermal performance of one-ended evacuated tubes for producing hot air, *J. Sol. Energy*, 2013 (2013) 524715, doi: 10.1155/2013/524715.
- [8] H. Kargar Sharif Abad, M. Ghiasi, S. Jahangiri Mamouri, M.B. Shafii, A novel integrated solar desalination system with a pulsating heat pipe, *Desalination*, 311 (2013) 206–210.
- [9] G.M. Zaki, A. Al-Turki, M. Al-Fatani, Experimental investigation on concentrator-assisted solar-stills, *Int. J. Sol. Energy*, 11 (1992) 193–199.
- [10] O.O. Badran, H.A. Al-Tahaine, The effect of coupling a flat-plate collector on the solar still productivity, *Desalination*, 183 (2005) 137–42.
- [11] N. Rahbar, J.A. Esfahani, Experimental study of a novel portable solar still by utilizing the heat pipe and thermoelectric module, *Desalination*, 284 (2012) 55–61.
- [12] A. Kasaeian, A.T. Eshghi, M. Sameti, A review on the applications of nanofluids in solar energy systems, *Renewable Sustainable Energy Rev.*, 43 (2015) 584–598.
- [13] S.A. Kalogirou, Solar thermal collectors and applications, *Prog. Energy Combust. Sci.*, 30 (2004) 231–295.
- [14] P. Durkaieswaran, K. Kalidasa Murugavel, Various special designs of single basin passive solar still – a review, *Renewable Sustainable Energy Rev.*, 49 (2015) 1048–1060.
- [15] H.E.S. Fath, M. El-Samanoudy, K. Fahmy, A. Hassabou, Thermal-economic analysis and comparison between pyramid-shaped and single-slope solar still configurations, *Desalination*, 159 (2003) 69–79.
- [16] V. Velmurugan, M. Gopalakrishnan, R. Raghu, K. Srithar, Single basin solar still with fin for enhancing productivity, *Energy Convers. Manage.*, 49 (2008) 2602–2608.
- [17] M.A. Samee, U.K. Mirza, T. Majeed, N. Ahmad, Design and performance of a simple single basin solar still, *Renewable Sustainable Energy Rev.*, 11 (2007) 543–549.
- [18] S. Kumar, G.N. Tiwari, Analytical expression for instantaneous exergy efficiency of a shallow basin passive solar still, *Int. J. Therm. Sci.*, 50 (2011) 2543–2549.
- [19] L.M. Ayompe, A. Duffy, M. Mc Keever, M. Conlon, S.J. McCormack, Comparative field performance study of flat plate and heat pipe evacuated tube collectors (ETCs) for domestic water heating systems in a temperate climate, *Energy*, 36 (2011) 3370–3378.
- [20] I. Budihardjo, G.L. Morrison, Performance of water-in-glass evacuated tube solar water heaters, *Sol. Energy*, 83 (2009) 49–56.
- [21] M.S. Hossain, R. Saidur, H. Fayaz, N.A. Rahim, M.R. Islam, J.U. Ahamed, M.M. Rahman, Review on solar water heater collector and thermal energy performance of circulating pipe, *Renewable Sustainable Energy Rev.*, 15 (2011) 3801–3812.
- [22] M.A. Sabiha, R. Saidur, S. Mekhilef, O. Mahian, Progress and latest developments of evacuated tube solar collectors, *Renewable Sustainable Energy Rev.*, 51 (2015) 1038–1054.
- [23] S.-Y. Yan, R. Tian, S. Hou, L.-N. Zhang, Analysis on unsteady state efficiency of glass evacuated solar collector with an inserted heat pipe, *J. Eng. Thermophys.*, 29 (2008) 323–326.
- [24] L. Xu, Z.F. Wang, G.F. Yuan, X. Li, Y. Ruan, A new dynamic test method for thermal performance of all-glass evacuated solar air collector, *Sol. Energy*, 86 (2012) 1222–1231.
- [25] J.T. Kim, H.T. Ahn, H.J. Han, H.T. Kim, W.G. Chun, The performance simulation of all-glass vacuum tubes with coaxial fluid conduit, *Int. Commun. Heat Mass Transfer*, 34 (2007) 587–597.
- [26] R.B. Liang, L.D. Ma, J.L. Zhang, D. Zhao, Theoretical and experimental investigation of the filled-type evacuated tube solar collector with U-tube, *Sol. Energy*, 85 (2011) 1735–1744.
- [27] J. Arturo Alfaro-Ayala, G. Martínez-Rodríguez, M. Picón-Núñez, A.R. Uribe-Ramírez, A. Gallegos-Muñoz, Numerical study of a low temperature water-in-glass evacuated tube solar collector, *Energy Convers. Manage.*, 94 (2015) 472–481.
- [28] Y. Kim, T. Seo, Thermal performances comparisons of the glass evacuated tube solar collectors with shapes of absorber tube, *Renewable Energy*, 32 (2007) 772–795.
- [29] H. Jafari Mosleh, S. Jahangiri Mamouri, M.B. Shafii, A. Hakim Sima, A new desalination system using a combination of heat pipe, evacuated tube and parabolic trough collector, *Energy Convers. Manage.*, 99 (2015) 141–150.
- [30] H.J. Han, J.T. Kim, H.T. Ahn, S.J. Lee, A three-dimensional performance analysis of all-glass vacuum tubes with coaxial fluid conduit, *Int. Commun. Heat Mass Transfer*, 35 (2008) 589–596.
- [31] A. Madduri, D. Loeder, N. Beutler, M. He, S. Sanders, Concentrated Evacuated Tubes for Solar-Thermal Energy Generation Using Stirling Engine, 2012 IEEE Energytech, IEEE, Cleveland, OH, USA, 2012, pp. 1–6.
- [32] Chr. Lamnatou, E. Papanicolaou, V. Belessiotis, N. Kyriakis, Experimental investigation and thermodynamic performance analysis of a solar dryer using an evacuated-tube air collector, *Appl. Energy*, 94 (2012) 232–243.

- [33] A. Fudholi, K. Sopian, M.H. Ruslan, M.A. Alghoul, M.Y. Sulaiman, Review of solar dryers for agricultural and marine products, *Renewable Sustainable Energy Rev.*, 14 (2010) 1–30.
- [34] R. Kumar, R.S. Adhikari, H.P. Garg, A. Kumar, Thermal performance of a solar pressure cooker based on evacuated tube solar collector, *Appl. Therm. Eng.*, 21 (2001) 1699–1706.
- [35] S.P. Vendan, L.P.A. Shunmuganathan, T.M. Kumar, C.S. Thanu, Study on design of an evacuated tube solar collector for high temperature steam generation, *Int. J. Emerging Technol. Adv. Eng.*, 2 (2012).
- [36] J.R. Mehta, M.V. Rane, Liquid desiccant based solar air conditioning system with novel evacuated tube collector as regenerator, *Procedia Eng.*, 51 (2013) 688–693.
- [37] M.I. Fadhel, K. Sopian, W.R.W. Daud, Performance analysis of solar-assisted chemical heat-pump dryer, *Sol. Energy*, 84 (2010) 1920–1928.
- [38] J.S. Gao, X. Ge, The Study of Solar Heat Pump with All-Glass Evacuated Tube, 2009 International Conference on Electrical Machines and Systems, IEEE, Tokyo, Japan, 2009, pp. 1–4.
- [39] A. Çağlar, C. Yamali, Performance analysis of a solar-assisted heat pump with an evacuated tubular collector for domestic heating, *Energy Build.*, 54 (2012) 22–28.
- [40] R. Shukla, K. Sumathy, P. Erickson, J.W. Gong, Recent advances in the solar water heating systems: a review, *Renewable Sustainable Energy Rev.*, 19 (2013) 173–190.
- [41] A. Sakhrieh, A. Al-Ghandoor, Experimental investigation of the performance of five types of solar collectors, *Energy Convers. Manage.*, 65 (2013) 715–720.
- [42] S. Rittidech, A. Donmaung, K. Kumsombut, Experimental study of the performance of a circular tube solar collector with closed-loop oscillating heat-pipe with check valve (CLOHP/CV), *Renewable Energy*, 34 (2009) 2234–2238.
- [43] G.L. Morrison, I. Budihardjo, M. Behnia, Water-in-glass evacuated tube solar water heater, *Sol. Energy*, 76 (2004) 135–140.
- [44] A.M. El-Nashar, Seasonal effect of dust deposition on a field of evacuated tube collectors on the performance of a solar desalination plant, *Desalination*, 239 (2009) 66–81.
- [45] E. Zambolin, D. Del Col, Experimental analysis of thermal performance of flat plate and evacuated tube solar collectors in stationary standard and daily conditions, *Sol. Energy*, 84 (2010) 1382–1396.
- [46] A.A. Al-Karaghoul, W.E. Alnaser, Performances of single and double basin solar-stills, *Appl. Energy*, 78 (2004) 347–354.
- [47] R. Schmid, R.E. Collins, B.A. Pailthorpe, Heat transport in Dewar-type evacuated tubular collectors, *Sol. Energy*, 45 (1990) 291–300.
- [48] L.D. Ma, Z. Lu, J.L. Zhang, R.B. Liang, Thermal performance analysis of the glass evacuated tube solar collector with U-tube, *Build. Environ.*, 45 (2010) 1959–1967.
- [49] A.W. Badar, R. Buchholz, F. Ziegler, Experimental and theoretical evaluation of the overall heat loss coefficient of vacuum tubes of a solar collector, *Sol. Energy*, 85 (2011) 1447–1456.
- [50] Z.Y. Li, C. Chen, H.L. Luo, Y. Zhang, Y.N. Xue, All-glass vacuum tube collector heat transfer model used in forced-circulation solar water heating system, *Sol. Energy*, 84 (2010) 1413–1421.
- [51] R. Tripathi, G.N. Tiwari, Effect of water depth on internal heat and mass transfer for active solar distillation, *Desalination*, 173 (2005) 187–200.
- [52] V.R. Dunkle, Solar Water Distillation; the Roof Type Still and the Multiple Effect Diffuser, International Developments in Heat Transfer, ASME, Part V University of Colorado, 1961.
- [53] A.Kr. Tiwari, G.N. Tiwari, Effect of water depths on heat and mass transfer in a passive solar still: in summer climatic condition, *Desalination*, 195 (2006) 78–94.
- [54] D.B. Singh, G.N. Tiwari, Effect of energy matrices on life cycle cost analysis of partially covered photovoltaic compound parabolic concentrator collector active solar distillation system, *Desalination*, 397 (2016) 75–91.
- [55] J. Ghaderian, N.A.C. Sidik, A. Kasaeian, S. Ghaderian, A. Okhovat, A. Pakzadeh, S. Samion, W.J. Yahya, Performance of copper oxide/distilled water nanofluid in evacuated tube solar collector (ETSC) water heater with internal coil under thermosyphon system circulations, *Appl. Therm. Eng.*, 121 (2017) 520–536.
- [56] G.N. Tiwari, R.K. Mishra, *Advanced Renewable Energy Sources*, Royal Society of Chemistry Publishing House, UK, 2012.
- [57] D.B. Singh, G.N. Tiwari, Exergoeconomic, enviroeconomic and productivity analyses of basin type solar stills by incorporating N identical PVT compound parabolic concentrator collectors: a comparative study, *Energy Convers. Manage.*, 135 (2017) 129–147.
- [58] R.V. Singh, S. Kumar, M.M. Hasan, M. Emran Khan, G.N. Tiwari, Performance of a solar still integrated with evacuated tube collector in natural mode, *Desalination*, 318 (2013) 25–33.
- [59] Y. Zhiqiang, G.L. Harding, B. Window, Water-in-glass manifolds for heat extraction from evacuated solar collector tubes, *Sol. Energy*, 32 (1984) 223–230.
- [60] S. Kumar, A. Dubey, G.N. Tiwari, A solar still augmented with an evacuated tube collector in forced mode, *Desalination*, 347 (2014) 15–24.
- [61] K. Sampathkumar, P. Senthilkumar, Utilization of solar water heater in a single basin solar still—an experimental study, *Desalination*, 297 (2012) 8–19.
- [62] Z.M. Omara, M.A. Eltawil, E.S.A. El Nashar, A new hybrid desalination system using wicks/solar still and evacuated solar water heater, *Desalination*, 325 (2013) 56–64.
- [63] S. Jahangiri Mamouri, H. Gholami Derami, M. Ghiasi, M.B. Shafii, Z. Shiee, Experimental investigation of the effect of using thermosyphon heat pipes and vacuum glass on the performance of solar still, *Energy*, 75 (2014) 501–507.
- [64] M. Yari, A.E. Mazareh, A.S. Mehr, A novel cogeneration system for sustainable water and power production by integration of a solar still and PV module, *Desalination*, 398 (2016) 1–11.
- [65] M.B. Shafii, M. Shahmohamadi, M. Faegh, H. Sadrhosseini, Examination of a novel solar still equipped with evacuated tube collectors and thermoelectric modules, *Desalination*, 382 (2016) 21–27.
- [66] S.W. Sharshir, G.L. Peng, N. Yang, M.A. Eltawil, M.K.A. Ali, A.E. Kabeel, A hybrid desalination system using humidification-dehumidification and solar stills integrated with evacuated solar water heater, *Energy Convers. Manage.*, 124 (2016) 287–296.
- [67] D.B. Singh, G.N. Tiwari, Energy, exergy and cost analyses of N identical evacuated tubular collectors integrated basin type solar stills: a comparative study, *Sol. Energy*, 155 (2017) 829–846.
- [68] G.L. Harding, Y. Zhiqiang, D.W. Mackey, Heat extraction efficiency of a concentric glass tubular evacuated collector, *Sol. Energy*, 35 (1985) 71–79.
- [69] L.J. Shah, S. Furbo, Vertical evacuated tubular-collectors utilizing solar radiation from all directions, *Appl. Energy*, 78 (2004) 371–395.
- [70] I. Budihardjo, G.L. Morrison, M. Behnia, Natural circulation flow through water-in-glass evacuated tube solar collectors, *Sol. Energy*, 81 (2007) 1460–1472.
- [71] J. Ghaderian, N.A.C. Sidik, An experimental investigation on the effect of Al_2O_3 /distilled water nanofluid on the energy efficiency of evacuated tube solar collector, *Int. J. Heat Mass Transfer*, 108 (2017) 972–987.
- [72] R.S. Tang, Y.Q. Yang, W.F. Gao, Comparative studies on thermal performance of water-in-glass evacuated tube solar water heaters with different collector tilt-angles, *Sol. Energy*, 85 (2011) 1381–1389.
- [73] R. Dev, G.N. Tiwari, Annual performance of evacuated tubular collector integrated solar still, *Desal. Water Treat.*, 41 (2012) 204–223.
- [74] X.R. Zhang, H. Yamaguchi, An experimental study on evacuated tube solar collector using supercritical CO_2 , *Appl. Therm. Eng.*, 28 (2008) 1225–1233.
- [75] M. Mahendran, G.C. Lee, K.V. Sharma, A. Shahrani, R.A. Bakar, Performance of evacuated tube solar collector using water-based titanium oxide nanofluid, *J. Mech. Eng. Sci.*, 3 (2012) 301–310.

- [76] N.A.C. Sidik, S. Samion, J. Ghaderian, M.N.A.W.M. Yazid, Recent progress on the application of nanofluids in minimum quantity lubrication machining: a review, *Int. J. Heat Mass Transfer*, 108 (2017) 79–89.
- [77] M. Shahi, A. Houshang Mahmoudi, F. Talebi, Numerical simulation of steady natural convection heat transfer in a 3-dimensional single-ended tube subjected to a nanofluid, *Int. Commun. Heat Mass Transfer*, 37 (2010) 1535–1545.
- [78] M.A. Sabiha, R. Saidur, S. Hassani, Z. Said, S. Mekhilef, Energy performance of an evacuated tube solar collector using single walled carbon nanotubes nanofluids, *Energy Convers. Manage.*, 105 (2015) 1377–1388.
- [79] S. Iranmanesh, H.C. Ong, B.C. Ang, E. Sadeghinezhad, A. Esmailzadeh, M. Mehrali, Thermal performance enhancement of an evacuated tube solar collector using graphene nanoplatelets nanofluid, *J. Cleaner Prod.*, 162 (2016) 121–129.
- [80] H.A. Hussain, Q. Jawad, K.F. Sultan, Experimental analysis on thermal efficiency of evacuated tube solar collector by using nanofluids, *Int. J. Sustainable Green Energy*, 4 (2015) 19–28.
- [81] Y.J. Tong, J.H. Kim, H.Y. Cho, Effects of thermal performance of enclosed-type evacuated U-tube solar collector with multi-walled carbon nanotube/water nanofluid, *Renewable Energy*, 83 (2015) 463–473.
- [82] A. Papadimitratos, S. Sobhansarbandi, V. Pozdin, A. Zakhidov, F. Hassani, Evacuated tube solar collectors integrated with phase change materials, *Sol. Energy*, 129 (2016) 10–19.
- [83] J.T. Kim, H.T. Ahn, H.J. Han, H.T. Kim, W.G. Chun, The performance simulation of all-glass vacuum tubes with coaxial fluid conduit, *Int. Commun. Heat Mass Transfer*, 34 (2007) 587–597.
- [84] H.N. Panchal, Enhancement of distillate output of double basin solar still with vacuum tubes, *J. King Saud Univ. – Eng. Sci.*, 27 (2015) 170–175.
- [85] L.M. Ayompe, A. Duffy, Thermal performance analysis of a solar water heating system with heat pipe evacuated tube collector using data from a field trial, *Sol. Energy*, 90 (2013) 17–28.
- [86] R.K. Mishra, V. Garg, G.N. Tiwari, Thermal modeling and development of characteristic equations of evacuated tubular collector (ETC), *Sol. Energy*, 116 (2015) 165–176.
- [87] D.B. Singh, G.N. Tiwari, Analytical characteristic equation of N identical evacuated tubular collectors integrated double slope solar still, *J. Sol. Energy Eng.*, 139 (2017) 1–11, doi: 10.1115/1.4036855.
- [88] J.L. Fernández, N. Chargoy, Multi-stage, indirectly heated solar still, *Sol. Energy*, 44 (1990) 215–223.
- [89] S. Toyama, K. Kangkuv, Gijitsu, Maruzen, Tokyo, 1972.
- [90] P.K. Nag, *Basic & Applied Thermodynamics*, Tata McGraw-Hill, 2004.
- [91] D.B. Singh, G.N. Tiwari, Performance analysis of basin type solar stills integrated with N identical photovoltaic thermal (PVT) compound parabolic concentrator (CPC) collectors: a comparative study, *Sol. Energy*, 142 (2017) 144–158.
- [92] D.B. Singh, G.N. Tiwari, I.M. Al-Helal, V.K. Dwivedi, J.K. Yadav, Effect of energy matrices on life cycle cost analysis of passive solar stills, *Sol. Energy*, 134 (2016) 9–22.
- [93] Shyam, G.N. Tiwari, I.M. Al-Helal, Analytical expression of temperature dependent electrical efficiency of N-PVT water collectors connected in series, *Sol. Energy*, 114 (2015) 61–76.

Appendix-A

$$(AF_R(\alpha\tau))_1 = PF_1 \alpha \tau^2 A_R F_R; \quad (AF_R U_L)_1 = (1 - K_k) \dot{m}_f C_f;$$

$$PF_1 = \frac{h_{pf}}{F' h_{pf} + U_{tpa}}; \quad U_L = \frac{U_{t,pa} h_{pf}}{F' h_{pf} + U_{t,pa}};$$

$$F_R = \frac{\dot{m}_f C_f}{U_L A_R} \left[1 - \exp\left(-\frac{2\pi r' L' U_L}{\dot{m}_f C_f}\right) \right];$$

$$K_k = \left(1 - \frac{A_R F_R U_L}{\dot{m}_f C_f} \right)$$

$$h_{pf} = 100 \text{ Wm}^2\text{K}^{-1}$$

$$U_{t,pa} = \left[\frac{R_{o2}}{R_{o1} h_i} + \frac{R_{o2} \ln\left(\frac{R_{i2}}{R_{i1}}\right)}{K_g} + \frac{1}{C_{ev}} + \frac{R_{o2} \ln\left(\frac{R_{o2}}{R_{o1}}\right)}{K_g} + \frac{1}{h_o} \right]^{-1}$$

The expressions for a_1 and $f_1(t)$ used in Eq. (40) and expressions of heat transfer coefficients used in Eqs. (36)–(39) are as follows:

$$a_1 = \frac{1}{M_w C_w} \left[\dot{m}_f C_f (1 - K_k^N) + U_s A_b \right];$$

$$f_1(t) = \frac{1}{M_w C_w} \left[\alpha'_{\text{eff}} A_b I_s(t) + \frac{(1 - K_k^N)}{(1 - K_k)} (AF_R(\alpha\tau))_1 I_b(t) + \left(\frac{(1 - K_k^N)}{(1 - K_k)} (AF_R U_L)_1 + U_s A_b \right) T_a \right];$$

$$\alpha'_{\text{eff}} = \alpha'_w + h_1 \alpha'_b + h'_1 \alpha'_g;$$

$$h_1 = \frac{h_{bw}}{h_{bw} + h_{ba}}; \quad h'_1 = \frac{h_{1w} A_g}{U_{c,ga} A_g + h_{1w} A_b}; \quad h_{1w} = h_{rwg} + h_{cwg} + h_{ewg};$$

$$h_{e,wg} = 16.273 \times 10^{-3} h_{c,wg} \left[\frac{P_w - P_{gi}}{T_w - T_{gi}} \right];$$

$$h_{c,wg} = 0.884 \left[(T_w - T_{gi}) + \frac{(P_w - P_{gi})(T_w + 273)}{268.9 \times 10^3 - P_w} \right]^{1/3};$$

$$P_w = \exp \left[25.317 - \frac{5,144}{T_w + 273} \right];$$

$$P_{gi} = \exp \left[25.317 - \frac{5,144}{T_{gi} + 273} \right];$$

$$h_{rwg} = (0.82 \times 5.67 \times 10^{-8}) \left[(T_w + 273)^2 + (T_{gi} + 273)^2 \right] \left[T_w + T_{gi} + 546 \right];$$

$$U_s = U_t + U_b; \quad U_b = \frac{h_{ba} h_{bw}}{h_{bw} + h_{ba}}; \quad U_t = \frac{h_{1w} U_{c,ga} A_g}{U_{c,ga} A_g + h_{1w} A_b};$$

$$U_{c,ga} = \frac{\frac{K_g}{l_g} h_{1g}}{\frac{K_g}{l_g} + h_{1g}}; \quad h_{ba} = \left[\frac{L_i}{K_i} + \frac{1}{h_{cb} + h_{rb}} \right]^{-1};$$

$$h_{cb} + h_{tb} = 5.7 \text{ Wm}^{-2}\text{K}^{-1}, h_{bw} = 100 \text{ Wm}^{-2}\text{K}^{-1};$$

The expressions for different terms used in double slope are as follows:

$$h_{1gE} = h_{rgE} + h_{cgE}$$

$$h_{1gW} = h_{rgW} + h_{cgW}$$

The expressions for a_1 and $f_1(t)$ used in Eq. (60) and expressions of heat transfer coefficients used in Eqs. (54)–(60) are as follows:

$$a_1 = \frac{1}{M_w C_w} \left[\frac{\dot{m}_f C_f (1 - K_k^N) + U_b A_b + \frac{h_{1wE} (P - A_2) A_b}{2P}}{\frac{h_{1wW} (P - B_2) A_b}{2P}} \right]$$

$$f_1(t) = \frac{1}{M_w C_w} \left[\left(\frac{\alpha'_w}{2} + h_1 \alpha'_b \right) A_b (I_{SE}(t) + I_{SW}(t)) + \frac{(1 - K_k^N)}{(1 - K_k)} (AF_R(\alpha\tau))_1 I(t) + \left(\frac{(1 - K_k^N)}{(1 - K_k)} (AF_R U_L)_1 + U_b A_b \right) T_a + \left(\frac{h_{1wE} A_1 + h_{1wW} B_1}{P} \right) \frac{A_b}{2} \right]$$

$$A_1 = R_1 U_1 A_{gE} + R_2 h_{EW} A_{gW}; \quad A_2 = h_{1wE} U_2 \frac{A_b}{2} + h_{EW} h_{1wW} \frac{A_b}{2};$$

$$P = \left(U_1 U_2 - \frac{h_{EW}^2}{A_{gE}} h_{1wW} \frac{A_b}{2} \right) A_{gW}; \quad U_1 = \frac{h_{1wE} \frac{A_b}{2} + h_{EW} A_{gE} + U_{c,gaE} A_{gE}}{A_{gW}}$$

$$U_2 = \frac{h_{1wW} \frac{A_b}{2} + h_{EW} A_{gW} + U_{c,gaW} A_{gW}}{A_{gE}}; \quad B_1 = \frac{(R_2 P + A_1 h_{EW}) A_{gW}}{U_2 A_{gE}}$$

$$B_2 = \frac{Ph_{1wW} \frac{A_b}{2} + h_{EW} A_{gW} A_2}{U_2 A_{gE}}; \quad R_1 = \alpha'_s I_{SE}(t) + U_{c,gaE} T_a;$$

$$R_2 = \alpha'_s I_{SW}(t) + U_{c,gaW} T_a$$

$$h_{EW} = 0.034 \times 5.67 \times 10^{-8} \left[(T_{giE} + 273)^2 + (T_{giW} + 273)^2 \right] \left[T_{giE} + T_{giW} + 546 \right]$$

$$U_{c,gaE} = \frac{\frac{K_g h_{1gE}}{l_g}}{\frac{K_g}{l_g} + h_{1gE}}; \quad U_{c,gaW} = \frac{\frac{K_g h_{1gW}}{l_g}}{\frac{K_g}{l_g} + h_{1gW}};$$

$$h_{1gE} = 5.7 + 3.8V; \quad h_{1gW} = 5.7 + 3.8V;$$

$$h_{1wE} = h_{rwgE} + h_{cwgE} + h_{ewgE};$$

$$h_{1wW} = h_{rwgW} + h_{cwgW} + h_{ewgW};$$

$$h_{ewgE} = 16.273 \times 10^{-3} h_{c,wgE} \left[\frac{P_w - P_{giE}}{T_w - T_{giE}} \right];$$

$$h_{cwgE} = 0.884 \left[(T_w - T_{giE}) + \frac{(P_w - P_{giE})(T_w + 273)}{268.9 \times 10^3 - P_w} \right]^{\frac{1}{3}};$$

$$h_{ewgW} = 16.273 \times 10^{-3} h_{c,wgW} \left[\frac{P_w - P_{giW}}{T_w - T_{giW}} \right];$$

$$h_{cwgW} = 0.884 \left[(T_w - T_{giW}) + \frac{(P_w - P_{giW})(T_w + 273)}{268.9 \times 10^3 - P_w} \right]^{\frac{1}{3}};$$

$$P_w = \exp \left[25.317 - \frac{5,144}{T_w + 273} \right]; \quad P_{giE} = \exp \left[25.317 - \frac{5,144}{T_{giE} + 273} \right];$$

$$P_{giW} = \exp \left[25.317 - \frac{5,144}{T_{giW} + 273} \right];$$

$$h_{rwgE} = (0.82 \times 5.67 \times 10^{-8}) \left[(T_w + 273)^2 + (T_{giE} + 273)^2 \right] \left[T_w + T_{giE} + 546 \right]$$

$$h_{rwgW} = (0.82 \times 5.67 \times 10^{-8}) \left[(T_w + 273)^2 + (T_{giW} + 273)^2 \right] \left[T_w + T_{giW} + 546 \right]$$